

**Task (g) Report, Contract 4D-5888-WTSA:  
Submitted for APM 227 –  
Report on Geographic and Seasonal Variability of  
Solar UV Radiation Affecting Human and Ecological Health**

**Elizabeth C. Weatherhead, PhD  
University of Colorado at Boulder**

**May, 2005  
Revised October, 2006**

**Report to the U.S. Environmental Protection Agency**

**Task (g)**

Compare the UV-B measurements with air pollution measurements to determine the effects of tropospheric air pollution on UV-B exposures.

These results have been peer-reviewed through a process supervised by EPA.

Cooperative Institute for Research in the Environmental Sciences  
University of Colorado at Boulder  
325 Broadway  
Boulder, CO 80305  
[betsy.weatherhead@colorado.edu](mailto:betsy.weatherhead@colorado.edu)  
+1 (303) 497 6653

<http://cires.colorado.edu/science/groups/weatherhead>

## EXECUTIVE SUMMARY

In 1995, the U.S. Environmental Protection Agency's Ultraviolet Monitoring Program began collecting data using Brewer instruments at various national park and urban sites. The dates of the Brewer network operation correspond with an interesting time in terms of changes in total column ozone and other parameters, including surface pollutants. This report analyzes the effects of near-surface ozone pollution levels on UV irradiance reaching Earth's surface. The analysis incorporates measurements from the Brewer network as well as from radiative transfer calculations to understand the effects of tropospheric ozone on UV transmission.

Recognizing that high surface ozone amounts can be detrimental to human health and to plants and other biological processes, the U.S. EPA has set air quality standards for ozone exposure during 8-hour and 1-hour periods. The 8-hour standard is 0.08 ppm (80 ppb). The 1-hr standard, which is being replaced with the 8-hr standard in most areas, is 0.12 ppm (120 ppb). The impacts of these two levels of surface ozone on UV reaching the surface are examined in this report.

Ozone throughout the atmosphere absorbs and therefore attenuates UV irradiance, though because of the small concentrations of ozone found in the lowest part of the atmosphere, the attenuation due to elevated surface ozone is often small compared to the attenuation from other factors. Analysis of collocated EPA Brewer measurements and surface ozone measurements for Chicago, Illinois, show a negative correlation between the two values, substantiating the idea that higher surface pollution can reduce the UV levels reaching the ground. Analyzing the Brewer data by wavelength shows an attenuation of 5 percent at the 305-nm wavelength and an attenuation of 3 percent at the 315-nm wavelength. This spectral dependence of the attenuation offers evidence that the UV attenuation is caused by ozone in the lower atmosphere, rather than by other atmospheric parameters such as clouds and aerosols, which absorb more consistently through the UV spectrum.

Radiative transfer calculations were performed for all 21 EPA Brewer locations using measured total column ozone values. Two high pollution situations were considered, corresponding to 80 ppb and 120 ppb of ozone in the lowest part of the atmosphere. The results of these calculations were compared to calculations that assumed no (0 ppb) boundary layer ozone. This comparison provides an estimate of the maximum effects of ozone in the lower atmosphere. The results across the network suggest that UV is generally attenuated by less than 5 percent for high ozone concentrations of 80 ppb. The attenuation is highest in the summer, with a network average of 3.9 percent, and lowest in the winter, with a network average of 2.9 percent. However, this maximum level is a comparison to no ozone in the surface layer. A comparison to actual background ozone levels would indicate enhanced surface ozone has a notably smaller impact on UV transmission.

## TABLE OF CONTENTS

1. Introduction and Background	page 4
2. Methods	page 7
<i>Data Quality Assurance</i>	page 7
<i>Modeling Pollutant Effects on UV</i>	page 12
3. Comparison of UV Irradiance and Air Quality at Chicago, Illinois	page 13
4. Detailed Site Analyses for All 21 Brewer Locations	page 19
5. Intercomparison of Results for All 21 Brewer Locations	page 41
6. Conclusion	page 48
7. References	page 50

## 1. Introduction and Background

Task (g) “compare the UV-B measurements with air pollution measurements to determine the effects of tropospheric air pollution on UV-B exposures” is one of several tasks defined by the U.S. Environmental Protection Agency (EPA) to analyze measurements from the network of ultraviolet radiation instruments operated by EPA and the University of Georgia (UGA) in collaboration with the National Park Service (NPS).

Other tasks address different elements of UV-B exposure and effects, and the results of those tasks are summarized in the individual task reports.

The tasks defined by the U.S. Environmental Protection Agency at the start of the project are as follows:

- (a) Determine the trends in UV-B flux at the individual Brewer sites, at groups of similar sites and/or across the network.
- (b) Analyze the factors affecting the observations and trends at each site (and across the network, as appropriate) including correlations with changes in the ozone column, changes in stratospheric ozone, changes in ground level ozone, changes attributable to other pollutants or atmospheric constituents, etc.
- (c) Analyze the major factors affecting the UV-B flux, including solar angle, latitude, elevation, cloud cover, pollution levels and composition, etc.
- (d) Analyze the direct versus indirect exposures to UV-B radiation and the factors affecting the ratio.
- (e) Compare the UV-B flux measurements with the predictions of the National Weather Service Ozone Watch Program, together with an analysis of the differences and potential causes for the discrepancies.
- (f) Compare the Brewer UV-B measurements with that of the Tropospheric Ultraviolet (TUV) Model, Total Ozone Mapping Spectrometer (TOMS) measurements, and provide an analysis of the differences of those measurements and the causes of those differences.
- (g) Compare the UV-B measurements with air pollution measurements to determine the effects of tropospheric air pollution on UV-B exposures.
- (h) Compare trends in UV-B flux measured by the network at mid-latitudes in the United States to United National Environmental Program (UNEP) data.
- (i) Determine the effect of clouds/haze/aerosols on UV-B exposure.

(j) Analyze the directional diffuse (cloudless) sky irradiance in the 290-325 nm (UV-B and 325-400nm (UV-A) wavelength bands as a function of aerosol optical depth.

(k) Analyze the directional diffuse sky irradiance in the 290-400nm (UV-B and UV-A) wavelength band as a function of cloud cover, cloud type, cloud depth.

(l) Analyze the reflectance (spectral albedo) for key materials (snow, beach sand, concrete, asphalt and water) in the 290nm-400nm (UV-B and UV-A) wavelength band, as appropriate for the network measurement sites.

(m) Analyze the bi-directional reflectance (forward-scattering and back-scattering) for key materials (snow, beach sand, concrete, asphalt and water) in the 290nm – 400nm (UV-B and UV-A) wavelength band, as appropriate for the network.

Task (g) analyzes the effects of air pollution on UV-B radiation reaching Earth's surface. Tropospheric ozone and other pollutants can absorb UV-B radiation and prevent a portion from reaching the surface. Increased air pollution levels have been observed to decrease surface erythemal UV by as much as 30 to 40 percent (Papayannis et al., 1998; Repapis et al., 1998). However, the effects of pollutants generally tend to be much smaller in magnitude than the UV impacts from changes in cloud or ozone amounts. Recent work quantifying the relative contributions to spectral transmission suggests that clouds in fact play a larger role than previously expected (Erlick and Frederick, 1998a; Erlick et al., 1998; Winiecki and Frederick, 2005).

For this analysis, the effects of pollutants are assessed using the U.S. EPA's standards for exposure during 8-hour and 1-hour periods. The 8-hour standard is 0.08 ppm (80 ppb), and locations are able meet attainment based on the three-year average of the 4th highest daily concentration. The 1-hr standard, which is being replaced with the 8-hr standard in most areas, is 0.12 ppm (120 ppb). Actual measurements of air pollution at the Brewer sites were not available, however, because of the Clean Air Act and its amendments, we expect the levels observed in the U.S. to be much less than those observed in developing countries. The near-surface levels of ozone at the Brewer locations are particularly low compared to levels in developing countries.

Because ultraviolet radiation drives the chemistry of the clean and polluted troposphere, it is important to understand the magnitude and variability of spectral UV irradiance reaching the ground as well as the mechanisms that control the transmission of UV through the atmosphere. Historically, much attention focused on the role of stratospheric ozone, although absorption and scattering in the troposphere are important as well. Specifically, in urban areas and regions downwind from them, elevated levels of gaseous and other absorbers, including black carbon, can provide enhanced attenuation of surface UV (Bruel and Crutzen, 1989; Erlick and Frederick, 1998b; Wenny et al., 2001); the magnitude of this effect is highly dependent on the prevailing air quality. More recently,

Barnard et al. (2003) showed that black carbon could result in as much as 35% attenuation of Diffey weighted UV. This work was done using Brewer data from California along with TOMS ozone data from satellite and aerosol data.

The objective of the present analysis is to assess the role of air quality in influencing ground-level ultraviolet irradiance in the spectral region of strong absorption by ozone at wavelengths shorter than 320 nm. Excess absorption of ultraviolet radiation associated with tropospheric ozone depends on the perturbation to the column amount associated with degraded air quality. In practice, this vertically integrated quantity is not measured. Instead, the local mixing ratio for ozone at the ground serves as a proxy for the addition to the ozone column. The implicit, and reasonable, assumption is that the mixing ratio is positively correlated with the appropriate change in the column, a value that is confined to the lowest one to two kilometers of the atmosphere.

## 2. Methods

### Quality Assurance

The first step in the analysis of the spectral UV data involved a review of the available data with the scientists at UGA to determine any potential biases at particular sites. UGA personnel have put considerable effort into producing a Level 1 data product suitable for scientific use. The Level 1 data from all 21 sites were used to address several questions about the various factors influencing UV. The spectral nature of the Brewer data, as well as the large geographic coverage of the Brewer network (Figure 1), allow for an analysis of changes in UV at various wavelengths, which can provide important information about the factors affecting UV throughout the continental United States and in Alaska and Hawaii.

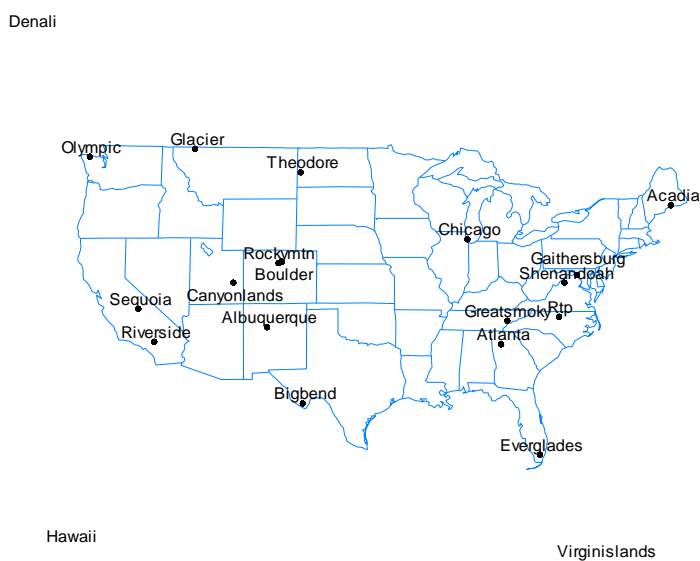


**Figure 1. The locations of instruments for the EPA Brewer UV monitoring network operated by the University of Georgia. The sites cover a large geographical area and represent a range of ecosystems.**

Parameters relating to UV observations and temperature characterizations at each of the Brewer sites are summarized in Table 1. Columns a through c give the latitude, longitude, elevation, and year observations were begun at each site.

Table 1. Location information for each of the Brewer instruments in the U.S. EPA UV Monitoring Network.

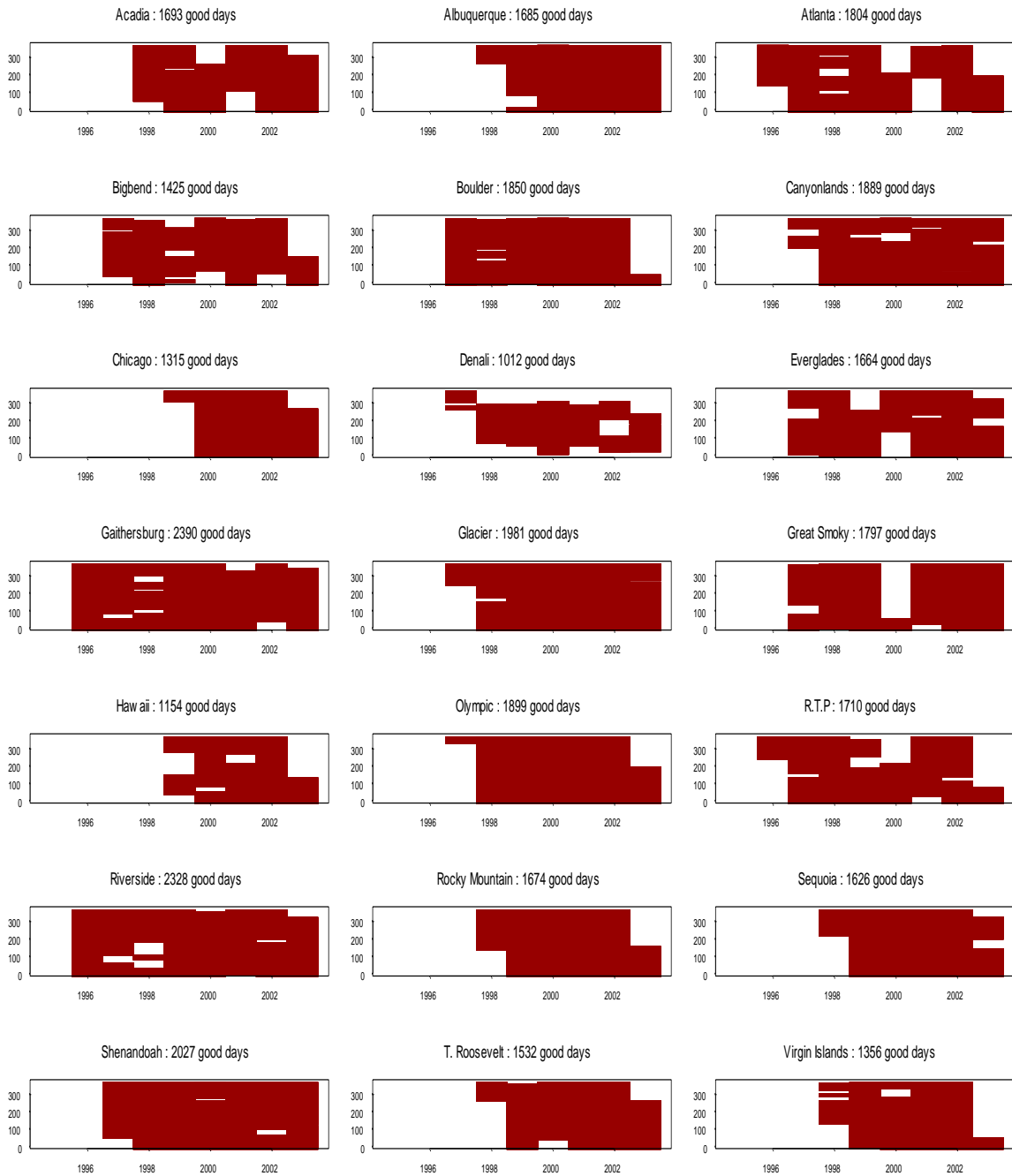
Site (Brewer #)	(a) Latitude/ Longitude	(b) Elevation	(c) Start Date
Glacier National Park, Montana (96-134)	48.7°N, 113.4°W	424 m	1997
Denali National Park, Alaska (96-141)	63.7°N, 149.0°W	661 m	1997
Olympic National Park, Washington (96-147)	48.1°N, 123.4°W	32 m	1997
Rocky Mountain National Park, Colorado (96-146)	40.0°N, 105.5°W	2896 m	1998
Hawaii Volcanoes National Park, Hawaii	19.4°N, 155.3°W	1243 m	1999
Boulder, CO (93-101)	40.1°N, 105.2°W	1689 m	1996
Gaithersburg, MD (105)	39.1°N, 77.2°W	43 m	1994
Acadia National Park, Maine (96-138)*	44.4°N, 68.3°W	137 m	1998
Everglades National Park, Florida (96-135) *	25.4°N, 80.7°W	18 m	1997
Chicago, IL (94-103)	41.8°N, 87.6°W	165 m	1999
Atlanta, GA (94-108) *	33.8°N, 84.4°W	91 m	1994
Research Triangle Park, NC (92-087)	35.9°N, 78.9°W	104 m	1995
Great Smoky National Park, TN (96-132) *	35.6°N, 83.8°W	564 m	1996
Big Bend National Park, Texas (96-130)	29.3°N, 103.2°W	329 m	1997
Albuquerque, NM (94-109) *	35.1°N, 106.6°W	1615 m	1998
Sequoia National Park, California (96-139) *	36.5°N, 118.8°W	549 m	1998
Virgin Islands National Park, U.S. Virgin Islands (96-144)	18.3°N, 64.8°W	30 m	1998
Shenandoah National Park, VA (96-137)	38.5°N, 78.4°W	325 m	1997
Canyonlands National Park, Utah (96-133)	38.5°N, 109.8°W	814 m	1997
Riverside, CA (94-112)	34.0°N, 117.3°W	84 m	1995
Theodore Roosevelt National Park, North Dakota (96-131) *	46.9°N, 103.4°W	238 m	1998

\*A site that has a shift or other problem

Problem values in the data, including missing scans or extremely high or low points, have been flagged in the Level 1 data files released by UGA. However, examination of the data has identified suspicious values that had not been flagged. The occurrence of such values varies from site to site, with some sites achieving extremely good collection rates

as well as high data quality. The results of extensive quality screening of the data are summarized in Figure 2. The data shown in red for each day have been evaluated as being problem-free, based on set criteria. Over 35,000 days of data have been identified as good: each of these “good” days contains between 10 and 50 UV scans.

# FLAGS - IDENTIFIED AS GOOD DAYS



Weatherhead Sun Sep 26 14:43:03 UMS 2004 task1.SSC

**Figure 2. The data presented here are as released on the University of Georgia web site and screened for quality. These data are used in this report to examine spectral UV changes over the time periods of instrument operation.**

The UGA staff screened the data based on the two criteria listed in the “readme” file associated with the site. The two criteria suggested for screening were that the data compared reasonably well to a clear sky model and that approximately the right number of scans was taken on a given day.

In addition to the screening performed by UGA as discussed above, we employed at least seven additional criteria. These additional criteria eliminated roughly 12 percent of the daily values. The checks were necessary to prevent systematic problems which could have had large impacts on the results presented. However, detailed screening of the spectral data was not possible and it is likely that some critical problems still exist in the individual spectral values.

The additional quality assurance tests are summarized as follows:

Test 1: The data were checked to define the time of the first scan. For the daily data to pass this test, the first scan had to have occurred within one hour of when the first scan was scheduled to occur.

Test 2: The data were checked to define the time of the last scan. For the daily data to pass this test, the last scan had to have occurred within one hour of when the last scan was scheduled to occur.

Test 3: The minimum solar zenith angles were checked. This test verifies whether scans were taken near solar noon. For the daily data to pass this test, the minimum solar zenith angle recorded was required be within three degrees of the expected solar zenith angle for that time of year.

Test 4: The number of scans in a single day was checked. This test evaluates whether enough data were taken to provide a reasonable estimate of the daytime-integrated value. The criterion for this test is that the number of scans must not differ from the scheduled number of scans for the time of year by more than 10.

Test 5: The data were visually evaluated for spikes. Spikes are a well-known phenomenon with the Brewer instruments, though their causes are not completely understood. Spikes result in extremely large values for single wavelength measurement in a single scan and do not represent a robust measurement of atmospheric composition. Many spikes had already been removed through UGA’s screening of the data.

Test 6: The data were assessed for problems with inappropriate time sequences. Occasionally, the data were written to files incorrectly, with two days of data recorded to one daily file. In these cases, the daytime-integrated UV was observed to be much higher than usual. We identified and screened these instances by looking for cases in which the

order of the solar zenith angles was out of line with what would happen during a normal day. The test also looked for uneven or highly irregular sampling during a day.

Test 7: The data were checked to assure that DUV values were within range. Observed daytime-integrated UV values are rarely above 7000 Joules/meter<sup>2</sup>/day and should never be equal to zero, given the sensitivity and locations of the Brewer instruments. All reported values greater than 9000 and less than or equal to zero were omitted from further evaluation. No efforts were made to determine the cause of these unusual values, however an inspection of when they occurred at each site showed no patterns consistent with an atmospheric cause of the unusual values.

Data were required to pass all seven tests to be used in the analysis of the Diffey-weighted UV. The number of data points removed in the screening process represented only a small portion of the data collected (less than 15 percent network wide), but the screening was necessary because only a few unusual points have the ability to change the results of the analyses.

### **Modeling Pollutant Effects on UV**

The effects of pollutants, including surface ozone and SO<sub>2</sub>, are assessed using a radiative model. The model used in this task implements the Discrete-Ordinate-Method Radiative Transfer model (DISORT) developed by Knut Stamnes (Stamnes et al., 1988). DISORT is a multi-stream radiative transfer model able to quantify the transfer of radiation in a scattering and emitting plane-parallel atmosphere. An interface improving the model's suitability for UV applications was added by Sasha Madronich at the National Center for Atmospheric Research, and improved further by Nataly Chubarova at Moscow State University in Russia.

The model uses a reference Rayleigh profile to simulate the molecular atmosphere and provides output in 80 vertical layers at a resolution of 1 km. The standard atmosphere profile is the 1976 reference atmosphere, and ozone absorption coefficients are those developed by Molina and Molina (1986) for temperatures of 263 K and 298 K. Sulfur dioxide (SO<sub>2</sub>) values are from McGee and Burris and nitrogen dioxide (NO<sub>2</sub>) is based on Davidson. For our purposes, pollution is concentrated in the lowest 1 km at levels 50 percent of ground concentration.

In coordination with Nataly Chubarova, the model was run to quantify the sensitivity of the UV-B flux to changes in atmospheric pollutants. The default values used in the study were as follows:

Latitude	40° N
Solar zenith angle	60°
Elevation	sea level

Cloudiness	0%
Pollution	varied*
Ozone	340 DU

Boundary layer ozone was represented using the 8-hour federal standard for surface ozone. This level is 0.08 ppm or 80 ppb. The 1-hour federal standard of 0.12 ppm (120 ppb) is also used, although reports indicate that this standard is being replaced with the 8-hour standard in most areas. The effects of these ozone concentrations are compared with model simulations using 0 ppb ozone, and using the results, we can quantify the reduction in UV-B based on changing surface ozone concentrations.

### **3. Comparison of UV Irradiance and Air Quality at Chicago, Illinois**

Data from the Brewer spectrophotometer located in Chicago, at latitude 41.79°N and longitude 87.60°W, were analyzed for the period from May through September of 2001, an interval that spans the period when photochemical processes are most likely to create degraded urban air quality. We excluded 19 days from this set owing to instrument-related problems and potentially poor data quality. In addition, the analysis omits all data collected at solar zenith angles (SZAs) in excess of 62 degrees. This omission was selected as a precaution to avoid angular response errors in the sensor at high sun elevations. It also ensures comparability with irradiances computed by a radiative transfer model that accounts for a spherical atmosphere in an approximate manner. After the above editing, the final dataset consisted of 958 spectral scans covering solar times from 9:00 hours to 15:00 hours. Sixty degrees solar zenith angle is used to help control for the effect of changing sun angle. In a hemispherically isotropic approximation, roughly half of the diffuse radiation is greater than sixty degrees and half is less. The primary reason for the choice, however, is to make the results presented here relatable to other published studies.

The Cook County Division of Environmental Control operates a chemiluminescent ozone sensor from the roof adjacent to the site of the Brewer spectrophotometer. Figure 4 presents the hourly surface ozone data for the time period of the Brewer observations. The maximum observed mixing ratio is 89 parts per billion by volume (ppbv), with a mean value of 32.9 ppbv.

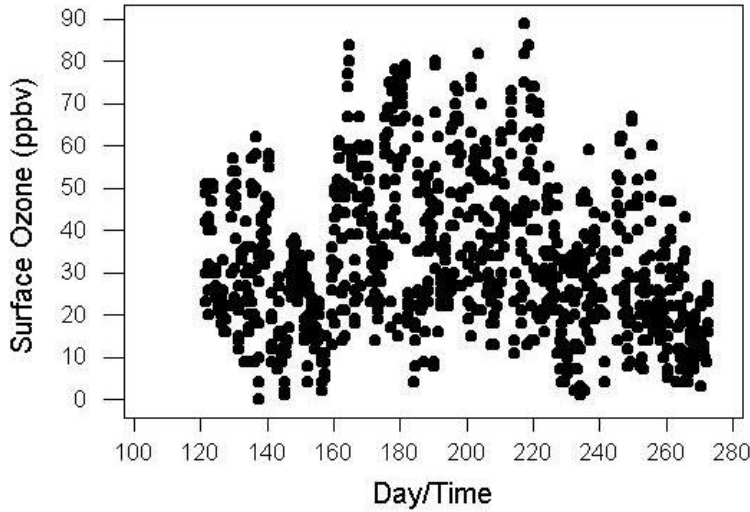


**Figure 4. Hourly surface ozone mixing ratios measured at the University of Chicago during the period of the Brewer Spectrophotometer observations. Values span solar times from 9:00 to 15:00 hours on each day.**

Solar ultraviolet irradiance received by a horizontal surface is a sensitive function of solar zenith angle (SZA), while radiation at wavelengths shorter than 320 nm varies inversely with the column ozone amount, approximately 90 percent of which resides in the stratosphere. Because this task focuses on absorption in the lower troposphere, it is important to develop a measure of ultraviolet irradiance that, for practical purposes, is independent of SZA and stratospheric ozone amounts. The "transmission ratio" is defined as:

$$T(\lambda) = E_M(\lambda, \theta) / E_C(\lambda, \theta, \Omega), \quad (1)$$

where  $E_M(\lambda, \theta)$  is the measured irradiance at wavelength  $\lambda$  in nm,  $\theta$  is the SZA,  $E_C(\lambda, \theta, \Omega)$  is the irradiance that would have existed under clear skies at the time of the measurement, and  $\Omega$  is the column ozone amount. In practice we use the radiative transfer model summarized by Frederick and Erlick (1995) with satellite-based column ozone measurements to compute a value of  $E_C(\lambda, \theta, \Omega)$  that pairs with each measured irradiance in the spectrophotometer's dataset. Care is required to ensure that the measured  $E_M(\lambda, \theta)$  and computed  $E_C(\lambda, \theta, \Omega)$  are indeed comparable since an offset between the absolute calibration of the spectrophotometer and the extraterrestrial solar irradiance used in the radiative transfer code will cause a bias in the transmission ratios. The techniques incorporated in our analysis allow for this possibility and automatically correct for any systematic offsets.

Ideally, values of  $T(\lambda)$  computed for wavelengths where ozone absorbs are still insensitive to the atmospheric ozone amount. This is the case when the value  $\Omega$  used to evaluate the denominator of equation 1 is identical to the true ozone amount to which the measured irradiance in the numerator responds. As noted below, attenuation by ozone in the urban boundary layer is implicit in the measured irradiances, but not in the computed irradiances in the denominator of equation 1. For the radiative transfer calculations we used daily values of column ozone deduced from NASA's Total Ozone Mapping Spectrometer (TOMS) carried on the Earth Probe satellite for the geographic location of the Brewer spectrophotometer. The data are available at <http://jwocky.gsfc.nasa.gov>. The solar backscatter method utilized by TOMS does not have high sensitivity to ozone located in the lower troposphere. The contribution functions at wavelengths absorbed by ozone undergo maxima in the lower stratosphere and are very small at altitudes below 5 km, even for clear skies. In addition, when clouds are present, the cloud top effectively acts as a lower atmospheric boundary as viewed from space. Column ozone values deduced from backscattered radiances measured by TOMS include contributions from the lower troposphere, but these are determined primarily by the ozone climatology input to the inversion algorithm rather than by information recorded by the sensor. Given this, we can consider the ozone abundance in the urban boundary layer to be a separate parameter, independent of the column ozone value contained in the database from TOMS.

We selected irradiances in four wavelength ranges from the Brewer spectrophotometer dataset for detailed analysis. These are the "305 nm band", defined as irradiance integrated over the range 303-308 nm, the "310 nm band" from 308-313 nm, the "315 nm band" from 313-318 nm, and the "345 nm band", encompassing 340-350 nm. Absorption by ozone is a major influence on ground-level irradiance in the 305 nm band, but decreases to become negligible in the longest wavelength region. The transmission ratios,  $T(305)$ ,  $T(310)$ ,  $T(315)$ , and  $T(345)$ , form the basis of the analysis reported here. Attenuation by clouds and aerosols determine the values of  $T(345)$ . The same processes influence the shorter wavelengths, but absorption by lower tropospheric ozone, that is not implicit in the TOMS column value used to compute  $E_C(\lambda, \theta, \Omega)$ , is also a factor.

Figure 5 is a histogram of the transmission ratios based on all irradiances measured in the 345 nm band, and Figure 6 presents the analogous results for the 305 nm band. Note that ratios in excess of 1.0 are possible when the sky is partly cloudy, but the solar disk is not obscured. Values in the range 0.7-1.0 are the most frequent, while ratios less than 0.7 occur in roughly one third of the observations. The total number of points that fall between 0.7 and 1.0 is very similar at each wavelength, although the smaller end of this range appears more frequently for the shorter wavelength band. The shift toward small values at the shorter wavelength suggests that a mechanism influences the 305 nm transmission that is absent at 345 nm, and absorption by ozone located in the boundary layer is a potential mechanism.

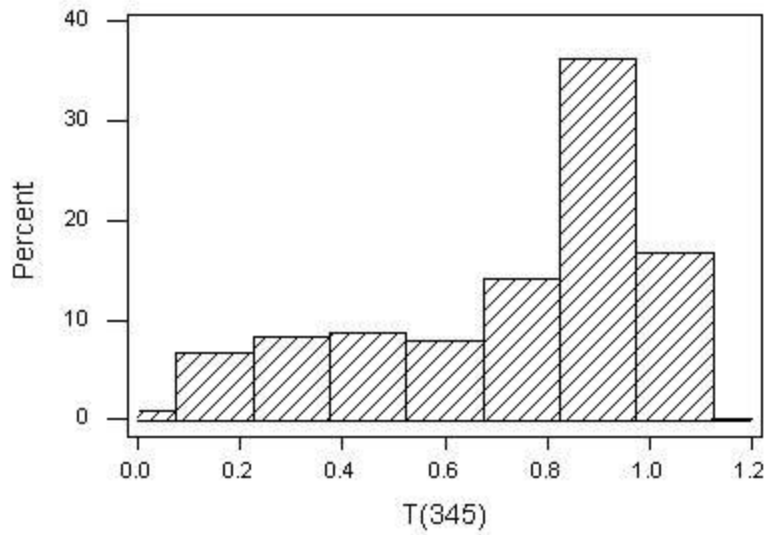


**Figure 5. Histogram of transmission ratios for the 345 nm band. The plot includes a total of 958 measurements at each wavelength.**

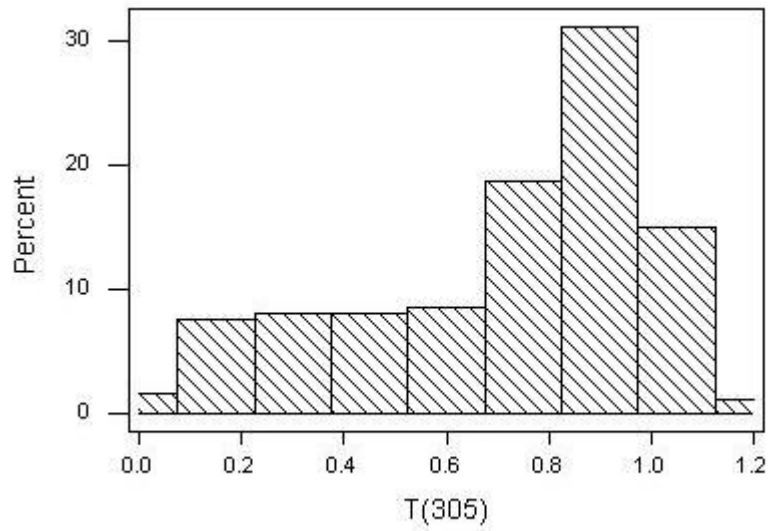


**Figure 6. Histogram of transmission ratios for the 305 nm band. The plot includes a total of 958 measurements at each wavelength.**

Clouds are by far the major influence on the shapes of the histograms in Figures 5 and 6, and it is necessary to account for this attenuation in order to isolate the much smaller effect of absorption by enhanced urban ozone amounts. A physically reasonable relationship between the transmission ratios and the mixing ratio of ozone,  $\chi$ , measured adjacent to the Brewer Spectrophotometer is:

$$T(\lambda) = \alpha T(345) \exp(-\beta\chi) \quad (2)$$

where  $\lambda = 305, 310, \text{ and } 315 \text{ nm}$ . This leads to a regression model of the form:

$$\ln[T(\lambda)/T(345)] = a - \beta\chi \quad (3)$$

where a value of "a" ( $=\ln \alpha$ ) that differs from 0.0 accounts for the presence of a systematic bias between  $T(\lambda)$  and  $T(345)$ .

The item of interest in this comparison is the value of  $\beta$ . If enhanced ozone amounts in a polluted urban boundary layer lead to a detectable attenuation of surface irradiance in, say, the 305 nm band, then one expects a positive value of  $\beta$  that differs significantly from 0.0. Physically, the value of  $\beta$  depends on the absorption cross section of ozone, the total number density of the atmosphere, and the vertical depth over which the excess ozone is distributed. The latter quantity will vary with time of day and meteorological conditions. Hence, while the results produced by the regression model will be valid in an averaged sense, the derived value of  $\beta$  may fail to describe conditions at any specific time.

We chose to restrict application of the regression model to skies that are nearly clear. This restriction is implemented because clouds provide can provide a much larger attenuation than do gaseous air pollutants, and their influence on the measured irradiances must be corrected-for in the analysis. Table 2 presents the results produced by the regression model of equation 3 when applied to all points for which  $T(345)>0.8$ . A total of 545 measurements meet this criterion. The estimated values of  $\beta$  are all positive, significantly different from zero, and vary with wavelength in a way similar to the absorption cross section of ozone (Molina and Molina, 1986). While the correlation of  $\ln[T(\lambda)/T(345)]$  with  $\chi$  is very significant, relatively little variance in the dependent variable is explained.

Table 2. Results of Applying the Regression Model " $\ln[T(\lambda)/T(345)] = a - \beta\chi$ " to Measurements where $T(345) > 0.8$ .			
Wavelength Band $\lambda$	Regression Coefficients	Standard Deviations	% Variance Explained
305 nm	$a = 4.011 \times 10^{-2}$ $\beta = 1.791 \times 10^{-3}$	$\sigma_a = 8.202 \times 10^{-3}$ $\sigma_\beta = 2.044 \times 10^{-4}$	12.4%
310 nm	$a = 3.613 \times 10^{-2}$ $\beta = 1.324 \times 10^{-3}$	$\sigma_a = 6.690 \times 10^{-3}$ $\sigma_\beta = 1.667 \times 10^{-4}$	10.4%
315 nm	$a = 2.557 \times 10^{-2}$ $\beta = 8.557 \times 10^{-4}$	$\sigma_a = 5.616 \times 10^{-3}$ $\sigma_\beta = 1.400 \times 10^{-4}$	6.4%

\* Read 0.943 as an irradiance equal to 94.3% of what would exist for a surface ozone mixing ratio equal to 0.

Based on the regression, a surface ozone mixing ratio  $\chi$  is accompanied by a reduction in ground-level irradiance to the fraction " $\exp(-\beta\chi)$ " of what would have existed for  $\chi=0.0$ , and it is convenient to characterize the influence of urban ozone by this exponential.

Table 3 present numerical values for  $\chi = 32.9$  ppbv, the average over the observing period, and  $\chi = 89$  ppbv, the maximum. An increase in surface ozone from 32.9 ppbv to 89 ppbv is accompanied (in a statistical sense) by reductions in irradiance of 9.5 percent for the 305 nm band, 7.1 percent for the 310 nm band, and 4.6 percent for the 315 nm band.

Table 3. Estimated Attenuation of Ultraviolet Irradiance by Urban Air Pollutants (based on regression results using ground-level ozone mixing ratios)*		
Wavelength Band	$\exp(-\beta\chi)$ $\chi = 32.9$ ppbv	$\exp(-\beta\chi)$ $\chi = 89$ ppbv
305 nm	0.943	0.853
310 nm	0.957	0.889
315 nm	0.972	0.927

In summary, the comparison of Brewer UV irradiances and air quality at Chicago, Illinois, reveals a readily detectable negative relationship between urban ozone amounts and ultraviolet irradiance received at the ground. Gaseous absorption is detectable because of its wavelength dependence. Scattering by urban aerosols and absorption by carbon-based particulates have little spectral signature. Their effects are implicit in the computed transmission ratios for the 345-nm band, and cannot be separated from the influence of thin clouds.

#### **4. Detailed Site Analyses For All 21 Brewer Locations**

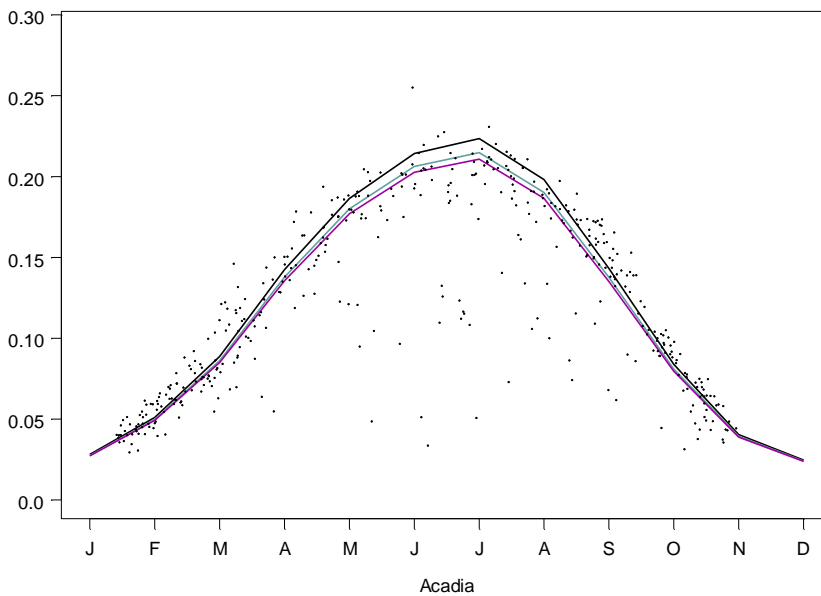
The following pages of plots present the results of the analyses for each Brewer instrument site. Each figure combines the results of the radiative transfer modeling with the Brewer UV measurements for that particular site. The effects of ozone pollution are illustrated by three curves: the black curve corresponds to modeled UV irradiances for 0 ppb surface ozone, the blue curve represents the modeled irradiance for 80 ppb surface ozone, and the purple curve corresponds to the modeled irradiance for 120 ppb surface ozone. From these curves, we are able to observe that as ozone concentration increases, the modeled amount of UV irradiance reaching the surface decreases.

# Acadia National Park

Latitude: 44.4°N  
Longitude: 68.3°W  
Elevation: 137 m



Influence of High Pollution Levels on Noontime UV



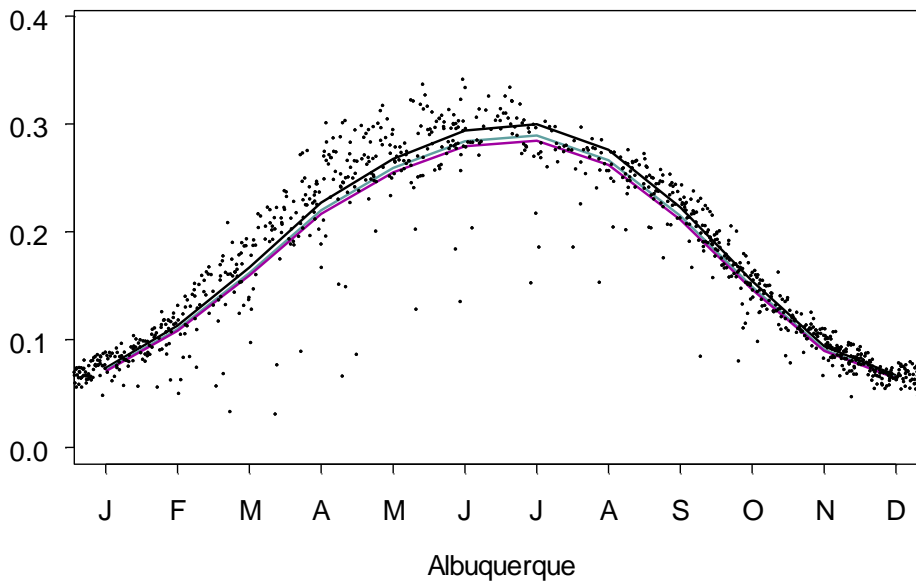
Acadia National Park is located in the northeastern U.S. The northern latitude location results in a very large seasonal cycle with the average UV in the summer more than eight times the average UV in the winter. The effects of ozone pollution are illustrated by the three curves in the above figure: the black curve corresponds to modeled UV irradiances for 0 ppb surface ozone, the blue curve represents the modeled irradiance for 80 ppb surface ozone, and the purple curve corresponds to the modeled irradiance for 120 ppb surface ozone. As ozone concentration increases, the amount of UV irradiance reaching the surface decreases. Each point in the figure represents the Brewer-measured UV irradiance at the site. The scatter in the points confirms that many factors besides pollution affect UV reaching the surface.

# Albuquerque, NM

Latitude: 35.1°N  
Longitude: 106.6°W  
Elevation: 1615 m



## Influence of High Pollution Levels on Noontime UV



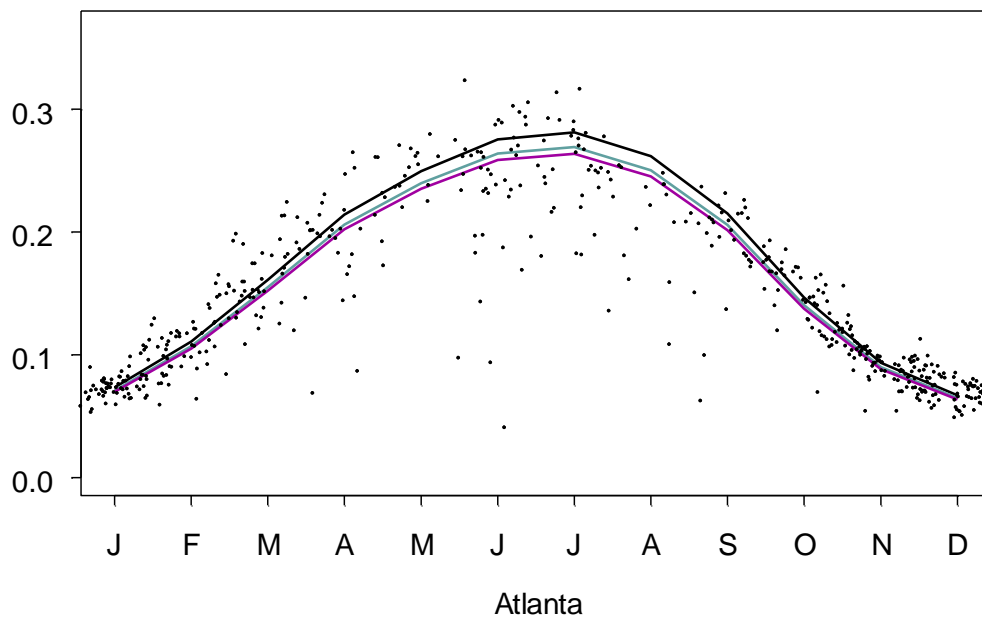
The metropolitan area of Albuquerque is known for its dry, hot climate in the summer and generally mild winters. The southern location and high elevation of the site results in extremes of UV levels. The effects of ozone pollution are illustrated by the three curves in the above figure: the black curve corresponds to modeled UV irradiances for 0 ppb surface ozone, the blue curve represents the modeled irradiance for 80 ppb surface ozone, and the purple curve corresponds to the modeled irradiance for 120 ppb surface ozone. As ozone concentration increases, the amount of UV irradiance reaching the surface decreases. The comparison assumes that all other values are held constant, which is not the case for the Brewer UV measurements, plotted as the small symbols in the figure. The scatter in the points confirms that many factors besides pollution affect UV reaching the surface, and suggests that the overall effects of pollution on UV irradiances are not large.

# Atlanta, GA

Latitude: 33.8°N  
Longitude: 84.4°W  
Elevation: 91 m



## Influence of High Pollution Levels on Noontime UV



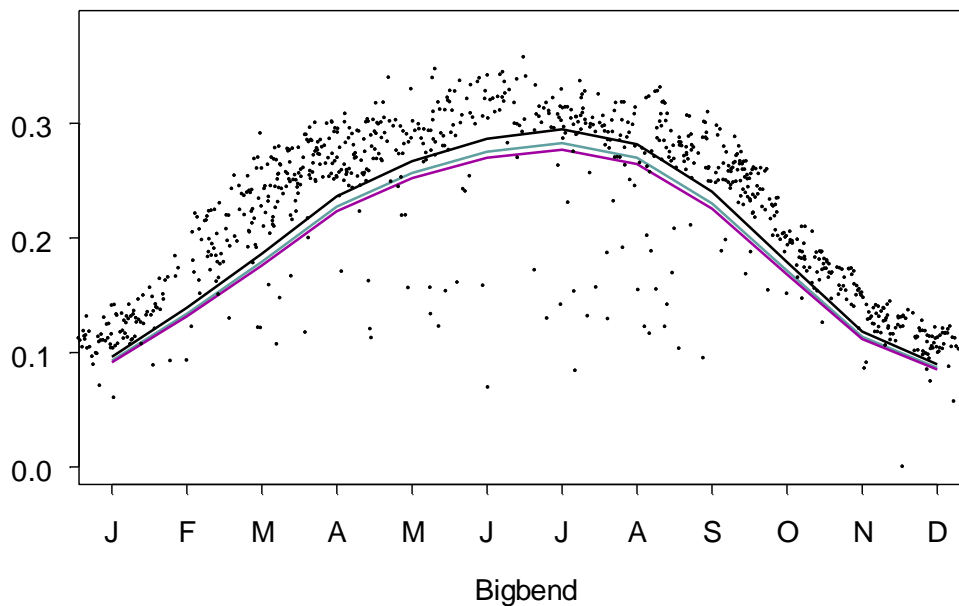
The twenty-county Atlanta metropolitan area is home to more than four million people and is an important urban monitoring site in the southern U.S. The effects of ozone pollution are illustrated by the three curves in the above figure: the black curve corresponds to modeled UV irradiances for 0 ppb surface ozone, the blue curve represents the modeled irradiance for 80 ppb surface ozone, and the purple curve corresponds to the modeled irradiance for 120 ppb surface ozone. As ozone concentration increases, the amount of UV irradiance reaching the surface decreases. The comparison assumes that all other values are held constant, which is not the case for the Brewer UV measurements, plotted as the small symbols in the figure. The scatter in the points confirms that many factors besides pollution affect UV reaching the surface, and suggests that the overall effects of pollution on UV irradiances are not large.

# Big Bend National Park

Latitude: 29.3°N  
Longitude: 103.2°W  
Elevation: 329 m



## Influence of High Pollution Levels on Noontime UV



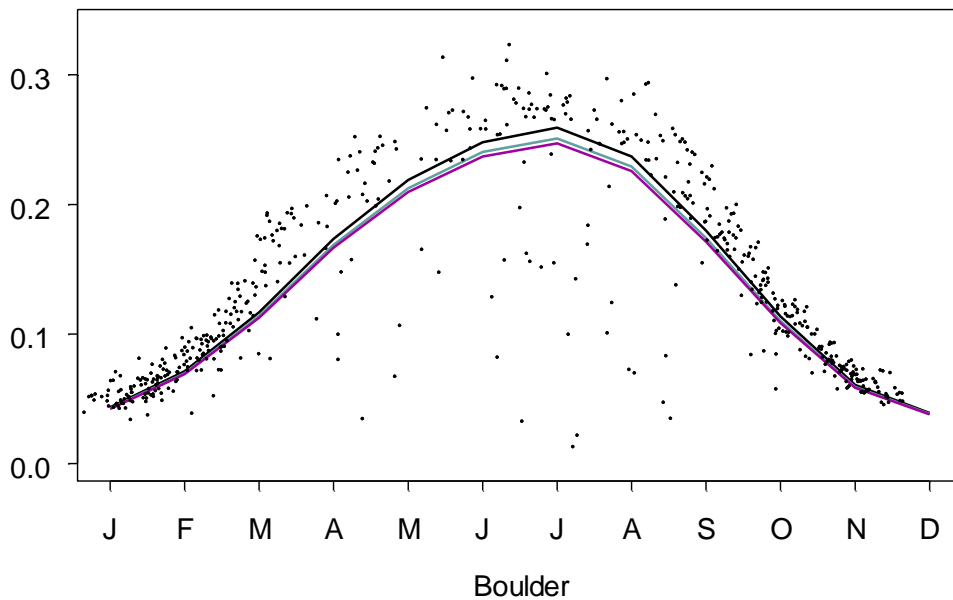
Big Bend National Park covers over 800,000 acres in southern Texas. The park hosts an array of ecological, paleontological, and archaeological research. The effects of ozone pollution are illustrated by the three curves in the above figure: the black curve corresponds to modeled UV irradiances for 0 ppb surface ozone, the blue curve represents the modeled irradiance for 80 ppb surface ozone, and the purple curve corresponds to the modeled irradiance for 120 ppb surface ozone. As ozone concentration increases, the amount of UV irradiance reaching the surface decreases. The comparison assumes that all other values are held constant, which is not the case for the Brewer UV measurements, plotted as the small symbols in the figure. The scatter in the points confirms that many factors besides pollution affect UV reaching the surface, and suggests that the overall effects of pollution on UV irradiances are not large.

# Boulder, CO

Latitude: 40.1°N  
Longitude: 105.2°W  
Elevation: 1689 m



## Influence of High Pollution Levels on Noontime UV



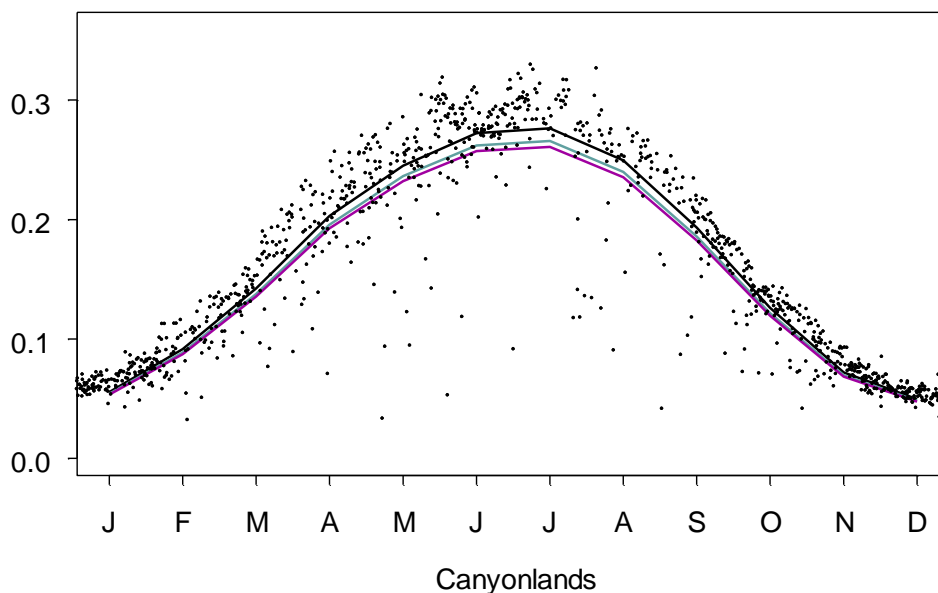
Boulder's UV monitoring takes place within 30 miles of the city of Denver at a fairly high elevation site. The effects of ozone pollution are illustrated by the three curves in the above figure: the black curve corresponds to modeled UV irradiances for 0 ppb surface ozone, the blue curve represents the modeled irradiance for 80 ppb surface ozone, and the purple curve corresponds to the modeled irradiance for 120 ppb surface ozone. As ozone concentration increases, the amount of UV irradiance reaching the surface decreases. The comparison assumes that all other values are held constant, which is not the case for the Brewer UV measurements, plotted as the small symbols in the figure. The scatter in the points confirms that many factors besides pollution affect UV reaching the surface, and suggests that the overall effects of pollution on UV irradiances are not large.

# Canyonlands National Park

Latitude: 38.5°N  
Longitude: 109.8°W  
Elevation: 814 m



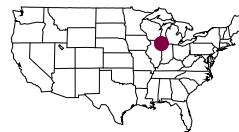
## Influence of High Pollution Levels on Noontime UV



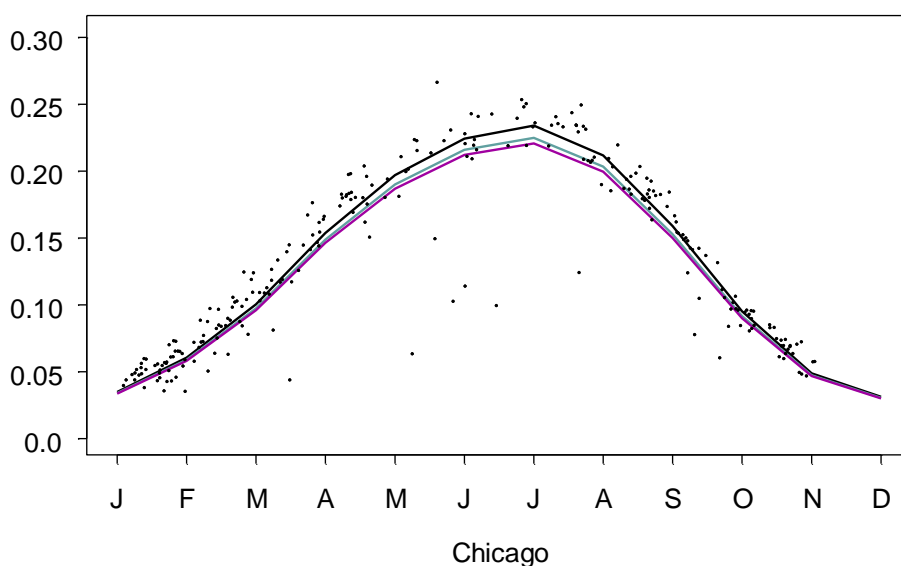
Canyonlands National Park is located in the high desert of Utah and is studied by numerous scientists because of its unique soil and a variety of algae, lichen, and bacteria that support a rich ecosystem. The effects of ozone pollution are illustrated by the three curves in the above figure: the black curve corresponds to modeled UV irradiances for 0 ppb surface ozone, the blue curve represents the modeled irradiance for 80 ppb surface ozone, and the purple curve corresponds to the modeled irradiance for 120 ppb surface ozone. As ozone concentration increases, the amount of UV irradiance reaching the surface decreases. The comparison assumes that all other values are held constant, which is not the case for the Brewer UV measurements, plotted as the small symbols in the figure. The scatter in the points confirms that many factors besides pollution affect UV reaching the surface, and suggests that the overall effects of pollution on UV irradiances are not large compared to other factors.

# Chicago, IL

Latitude: 41.8°N  
Longitude: 87.6°W  
Elevation: 165 m



## Influence of High Pollution Levels on Noontime UV



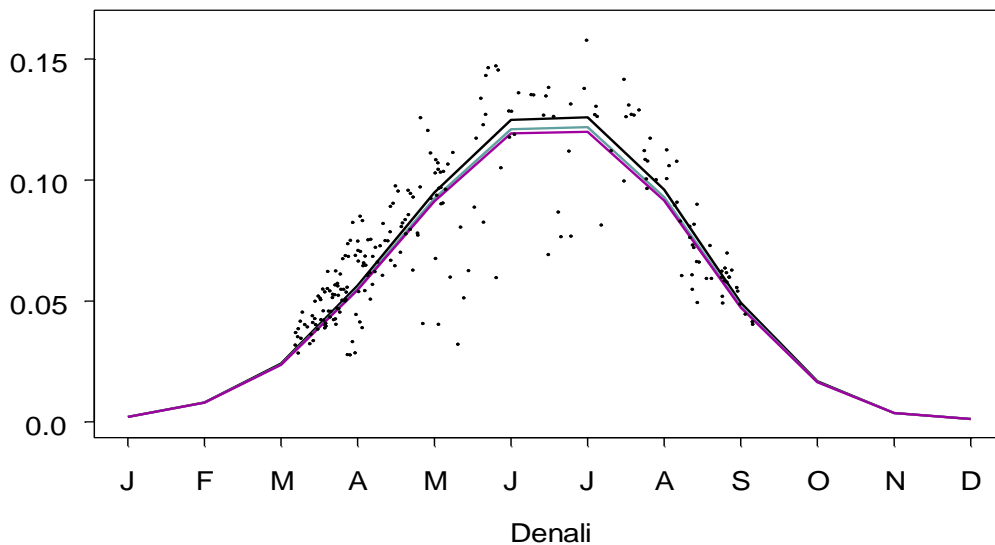
The nine-county metropolitan area of Chicago is located in the heart of the United States on the southern shore of Lake Michigan. The UV measurements represented here are taken on the University of Chicago campus and have been used extensively by John Frederick and several of his students. The effects of ozone pollution are illustrated by the three curves in the above figure: the black curve corresponds to modeled UV irradiances for 0 ppb surface ozone, the blue curve represents the modeled irradiance for 80 ppb surface ozone, and the purple curve corresponds to the modeled irradiance for 120 ppb surface ozone. As ozone concentration increases, the amount of UV irradiance reaching the surface decreases. The comparison assumes that all other values are held constant, which is not the case for the Brewer UV measurements, plotted as the small symbols in the figure. The scatter in the points confirms that many factors besides pollution affect UV reaching the surface, and suggests that changes in pollution concentrations have only a small effect on UV reaching the surface.

# Denali National Park

Latitude: 63.7°N  
Longitude: 149.0°W  
Elevation: 661 m



## Influence of High Pollution Levels on Noontime UV



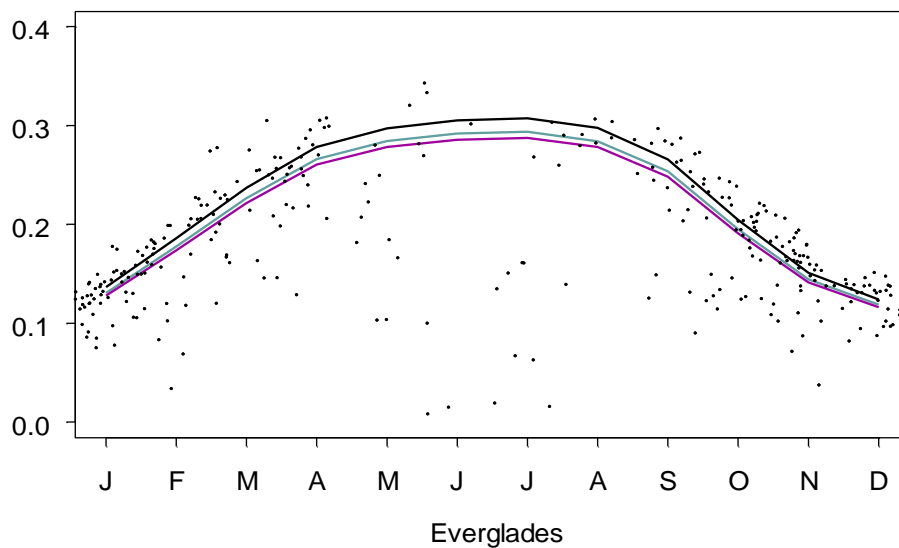
Denali National Park is the farthest north site in the EPA Brewer network. The data reflect a higher seasonality than those at any other site, with the winter values being generally quite low, often below the detection limit of the instrument. The effects of ozone pollution are illustrated by the three curves in the above figure: the black curve corresponds to modeled UV irradiances for 0 ppb surface ozone, the blue curve represents the modeled irradiance for 80 ppb surface ozone, and the purple curve corresponds to the modeled irradiance for 120 ppb surface ozone. As ozone concentration increases, the amount of UV irradiance reaching the surface decreases. The comparison assumes that all other values are held constant, which is not the case for the Brewer UV measurements, plotted as the small symbols in the figure. The scatter in the UV data confirms that many factors besides pollution affect UV reaching the surface. The overall effects of pollution on UV irradiances are not large compared to the effects of Sun angle, clouds, and other factors.

# Everglades National Park

Latitude: 25.4°N  
Longitude: 80.7°W  
Elevation: 18 m



## Influence of High Pollution Levels on Noontime UV



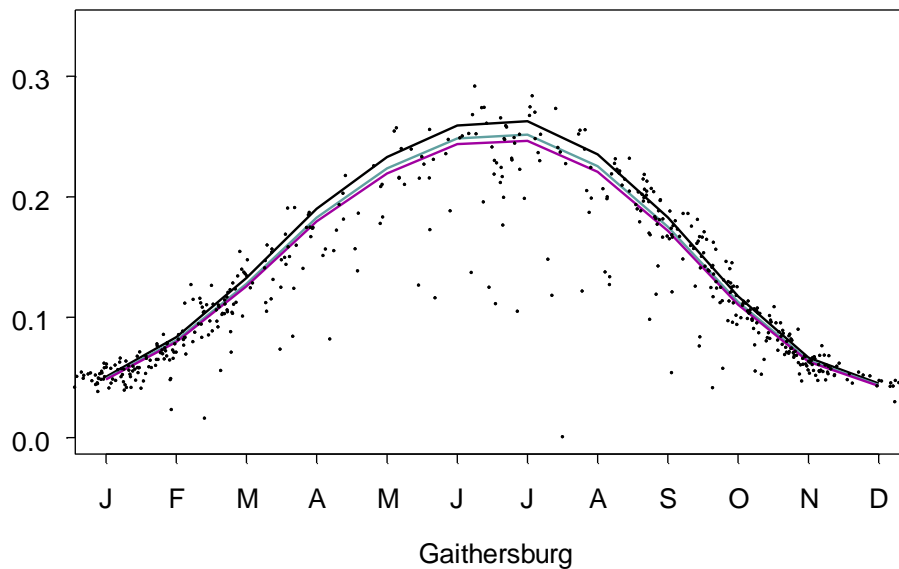
Everglades National Park encompasses more than 1.4 million acres and is host to over a million visitors each year. The busiest tourist season occurs during the winter months. As the data above show, the summer UV levels are higher than the winter levels by only a factor of 2. The effects of ozone pollution are illustrated by the three curves in the above figure: the black curve corresponds to modeled UV irradiances for 0 ppb surface ozone, the blue curve represents the modeled irradiance for 80 ppb surface ozone, and the purple curve corresponds to the modeled irradiance for 120 ppb surface ozone. As ozone concentration increases, the amount of UV irradiance reaching the surface decreases. The comparison assumes that all other values are held constant, which is not the case for the Brewer UV measurements, plotted as the small symbols in the figure. The scatter in the UV data confirms that many factors besides pollution affect UV reaching the surface. The overall effects of pollution on UV irradiances are not large compared to the effects of Sun angle, clouds, and other factors.

# Gaithersburg, MD

Latitude: 39.1°N  
Longitude: 77.2°W  
Elevation: 43 m



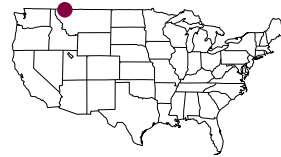
## Influence of High Pollution Levels on Noontime UV



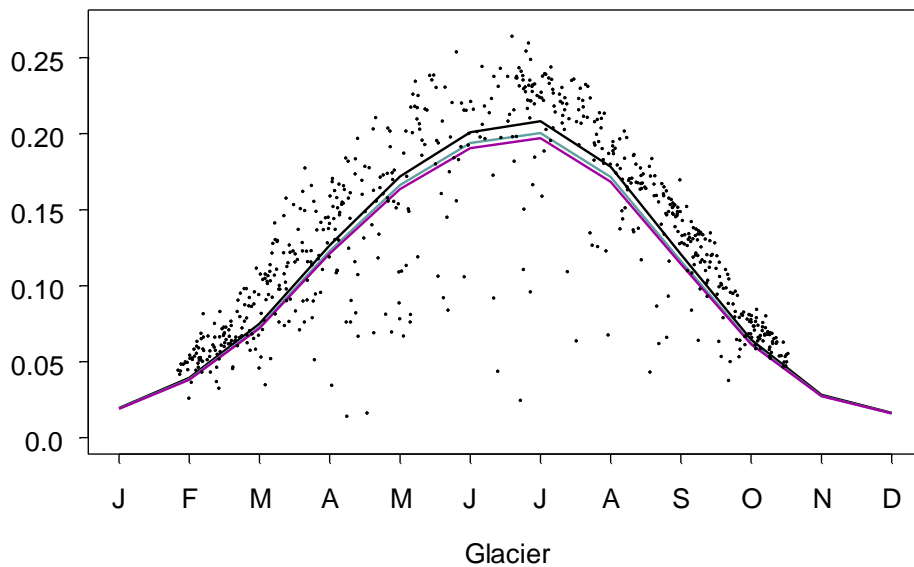
Gaithersburg, Maryland is located within 30 miles of both Baltimore, Maryland, and Washington, DC, in the eastern United States. The effects of ozone pollution are illustrated by the three curves in the above figure: the black curve corresponds to modeled UV irradiances for 0 ppb surface ozone, the blue curve represents the modeled irradiance for 80 ppb surface ozone, and the purple curve corresponds to the modeled irradiance for 120 ppb surface ozone. As ozone concentration increases, the amount of UV irradiance reaching the surface decreases. The comparison assumes that all other values are held constant, which is not the case for the Brewer UV measurements, plotted as the small symbols in the figure. The scatter in the points confirms that many factors besides pollution affect UV reaching the surface, and suggests that the overall effects of pollution on UV irradiances are not large.

# Glacier National Park

Latitude: 48.7°N  
Longitude: 113.4°W  
Elevation: 424 m



### Influence of High Pollution Levels on Noontime UV



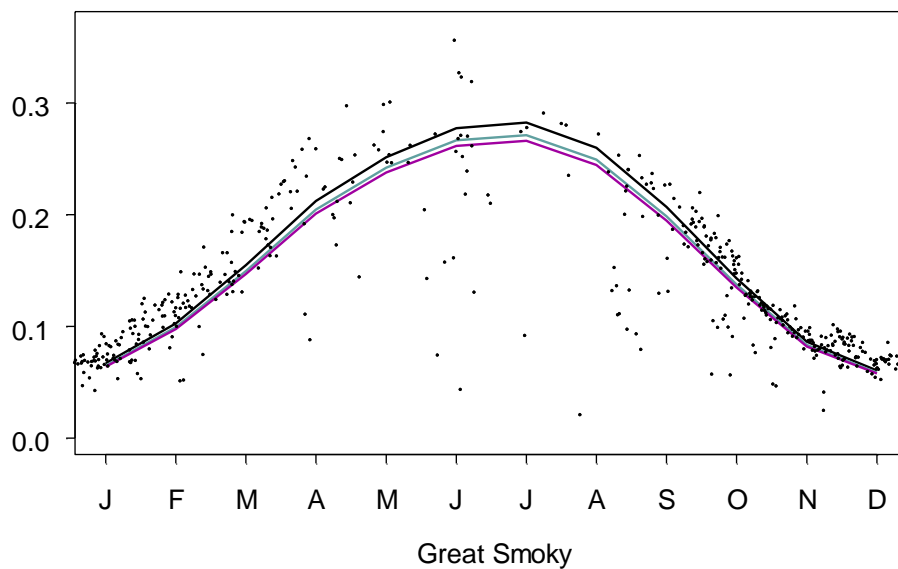
Glacier National Park encompasses over a million acres of land at high elevation in the northern U.S. The effects of ozone pollution are illustrated by the three curves in the above figure: the black curve corresponds to modeled UV irradiances for 0 ppb surface ozone, the blue curve represents the modeled irradiance for 80 ppb surface ozone, and the purple curve corresponds to the modeled irradiance for 120 ppb surface ozone. As ozone concentration increases, the amount of UV irradiance reaching the surface decreases. The comparison assumes that all other values are held constant, which is not the case for the Brewer UV measurements, plotted as the small symbols in the figure. The scatter in the points confirms that many factors besides pollution affect UV reaching the surface. In general, changing pollution concentrations do not strongly affect surface UV irradiance.

# Great Smoky Mountains National Park



Latitude: 35.6°N  
Longitude: 83.8°W  
Elevation: 564 m

## Influence of High Pollution Levels on Noontime UV



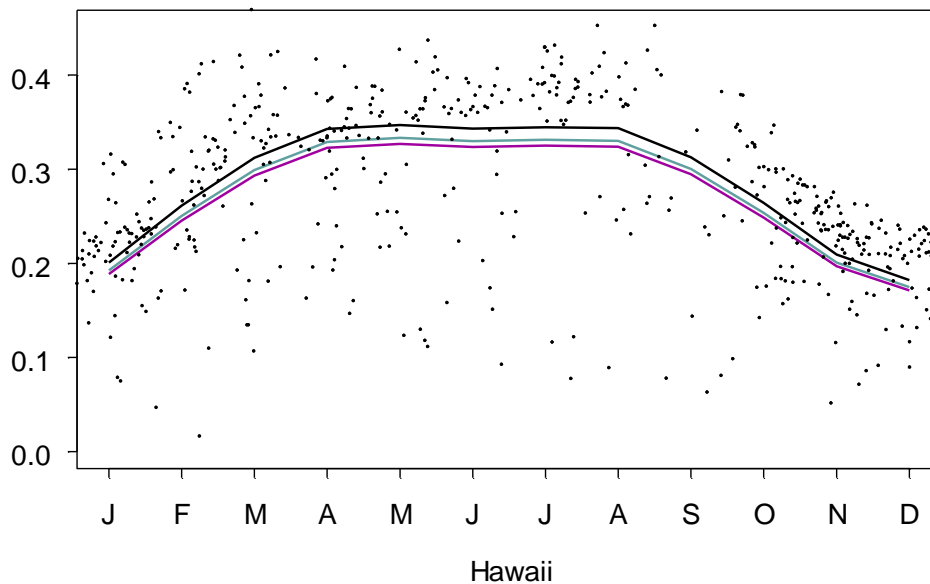
Great Smoky National Park encompasses over a half million acres of land in the southeastern U.S. The effects of ozone pollution are illustrated by the three curves in the above figure: the black curve corresponds to modeled UV irradiances for 0 ppb surface ozone, the blue curve represents the modeled irradiance for 80 ppb surface ozone, and the purple curve corresponds to the modeled irradiance for 120 ppb surface ozone. As ozone concentration increases, the amount of UV irradiance reaching the surface decreases. The comparison assumes that all other values are held constant, which is not the case for the Brewer UV measurements, plotted as the small symbols in the figure. The scatter in the points confirms that many factors besides pollution affect UV reaching the surface, and suggests that the overall effects of pollution on UV irradiances are not large.

# Hawaii Volcanoes National Park

Latitude: 19.42 °N  
Longitude: 155.28 °W  
Elevation: 1243 m



## Influence of High Pollution Levels on Noontime UV



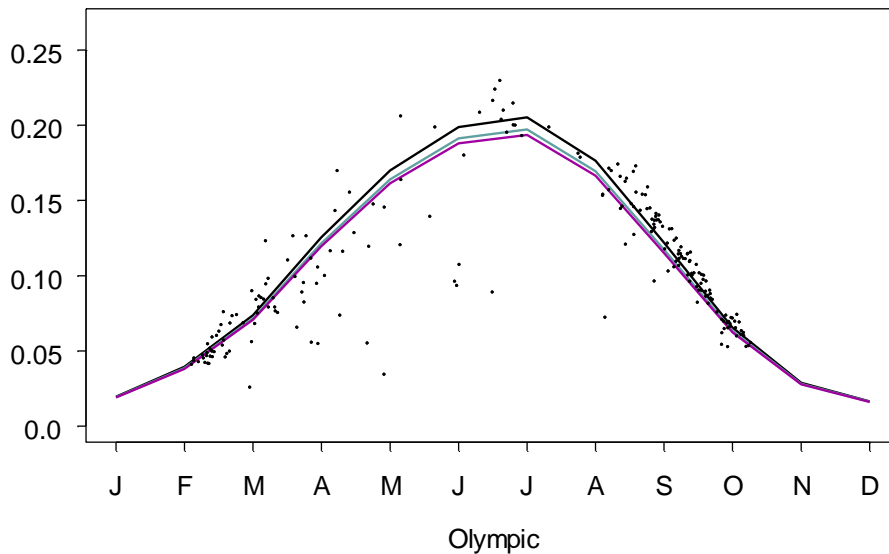
Hawaii Volcanoes National Park covers over 300,000 acres at a high elevation on a Pacific island. The effects of ozone pollution are illustrated by the three curves in the above figure: the black curve corresponds to modeled UV irradiances for 0 ppb surface ozone, the blue curve represents the modeled irradiance for 80 ppb surface ozone, and the purple curve is the modeled irradiance for 120 ppb surface ozone. As ozone concentration increases, the amount of UV irradiance reaching the surface decreases. The comparison assumes that all other values are held constant, which is not the case for the Brewer UV measurements, plotted as the small symbols in the figure. At this site, pollution affects are likely to be minimal. The large scatter in the UV values confirms that many factors other than pollution affect UV amounts at this location.

# Olympic National Park

Latitude: 48.1°N  
Longitude: 123.4°W  
Elevation: 32 m



## Influence of High Pollution Levels on Noontime UV



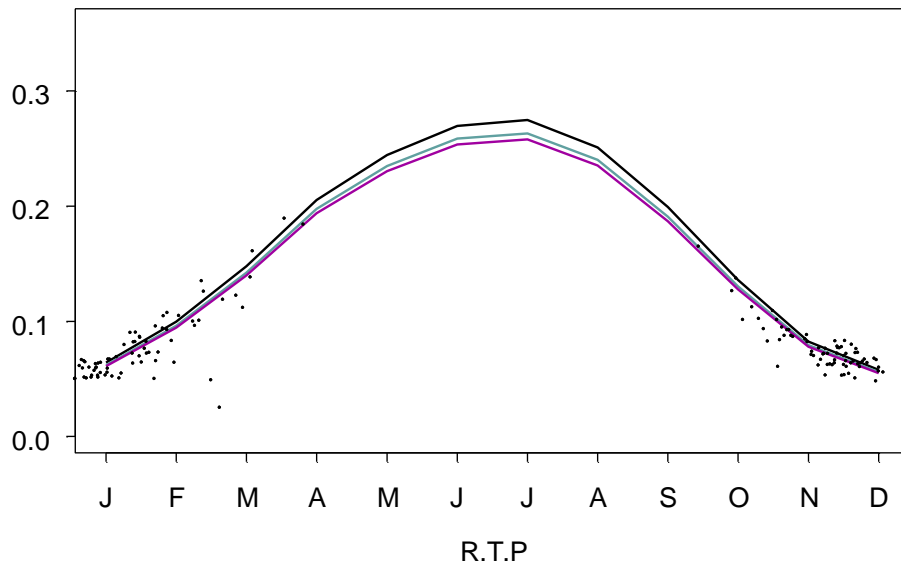
Olympic National Park encompasses over 900,000 acres in the northwestern U.S. It is one of the most northerly parks in the network and as such experiences a strong seasonal cycle in UV irradiance. The effects of ozone pollution are illustrated by the three curves in the above figure: the black curve corresponds to modeled UV irradiances for 0 ppb surface ozone, the blue curve represents the modeled irradiance for 80 ppb surface ozone, and the purple curve corresponds to the modeled irradiance for 120 ppb surface ozone. As ozone concentration increases, the amount of UV irradiance reaching the surface decreases. The comparison assumes that all other values are held constant, which is not the case for the Brewer UV measurements, plotted as the small symbols in the figure. Overall, the effects of changing pollutant concentrations are not likely to be large compared to the effects of other factors.

# Research Triangle Park

Latitude: 35.9°N  
Longitude: 78.9°W  
Elevation: 104 m



## Influence of High Pollution Levels on Noontime UV



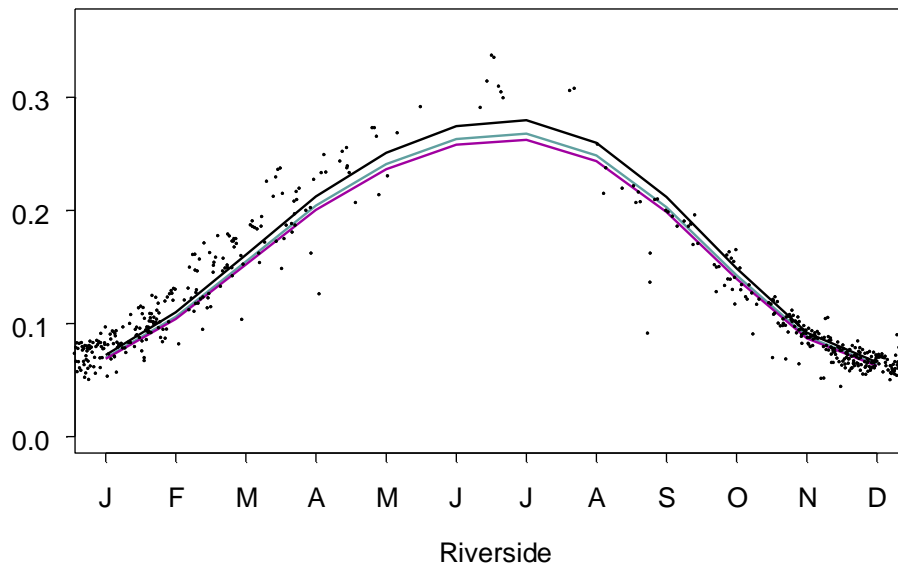
Research Triangle Park is one of the country's premier research areas in the eastern U.S. One of the first EPA network instruments was installed near RTP and the data from this site have been studied by a number of researchers. The effects of ozone pollution are illustrated by the three curves in the above figure: the black curve corresponds to modeled UV irradiances for 0 ppb surface ozone, the blue curve represents the modeled irradiance for 80 ppb surface ozone, and the purple curve corresponds to the modeled irradiance for 120 ppb surface ozone. As ozone concentration increases, the amount of UV irradiance reaching the surface decreases. The comparison assumes that all other values are held constant, which is not the case for the Brewer UV measurements, plotted as the small symbols in the figure. Many factors besides pollution affect UV reaching the surface, and the overall effects of pollution on UV irradiances are likely to be small.

# Riverside, CA

Latitude: 34.0°N  
Longitude: 117.3°W  
Elevation: 84 m



## Influence of High Pollution Levels on Noontime UV



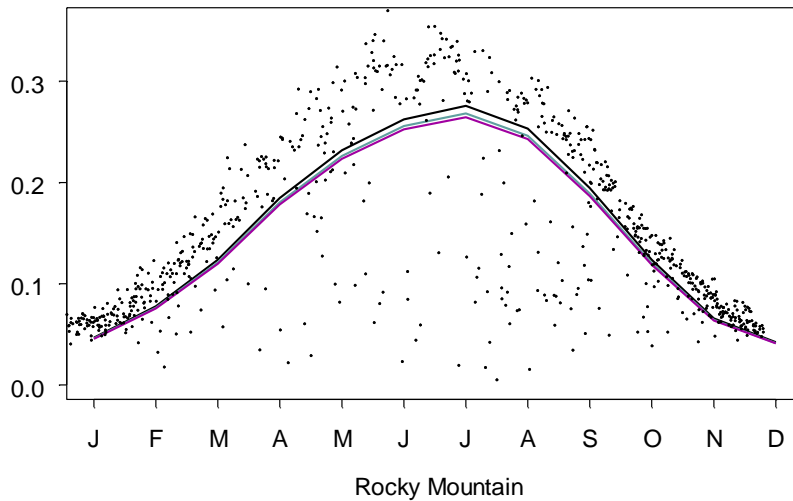
The Riverside-San Bernardino area is home to over 3.5 million people and is near the population area of Los Angeles which includes over 9 million people. The location is known both for its air pollution and its success in reducing pollution over the last decade. The effects of ozone pollution are illustrated by the three curves in the above figure: the black curve corresponds to modeled UV irradiances for 0 ppb surface ozone, the blue curve represents the modeled irradiance for 80 ppb surface ozone, and the purple curve corresponds to the modeled irradiance for 120 ppb surface ozone. As ozone concentration increases, the amount of UV irradiance reaching the surface decreases. The comparison assumes that all other values are held constant, which is not the case for the Brewer UV measurements, plotted as the small symbols in the figure. The scatter in the points confirms that many factors besides pollution affect UV reaching the surface, and suggests that the overall effects of pollution on UV irradiances are not large.

# Rocky Mountain National Park

Latitude: 40.0°N  
Longitude: 105.5°W  
Elevation: 2896 m



### Influence of High Pollution Levels on Noontime UV



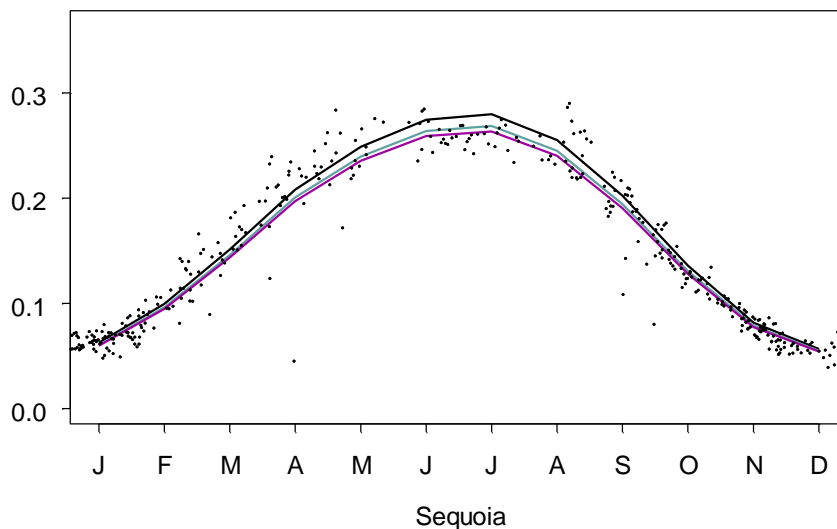
Rocky Mountain National Park is located at the high elevation site on the east side of the Rocky Mountains. Its high elevation results in a very strong seasonal cycle, while its mid-latitude location results in generally low variability compared to other sites. The effects of ozone pollution are illustrated by the three curves in the above figure: the black curve corresponds to modeled UV irradiances for 0 ppb surface ozone, the blue curve represents the modeled irradiance for 80 ppb surface ozone, and the purple curve corresponds to the modeled irradiance for 120 ppb surface ozone. As ozone concentration increases, the amount of UV irradiance reaching the surface decreases. The comparison assumes that all other values are held constant, which is not the case for the Brewer UV measurements, plotted as the small symbols in the figure. The scatter in the points confirms that many factors besides pollution affect UV reaching the surface, and suggests that the overall effects of pollution on UV irradiances are not large, particularly in higher elevation areas.

# Sequoia National Park

Latitude: 36.5°N  
Longitude: 118.8°W  
Elevation: 549 m



## Influence of High Pollution Levels on Noontime UV



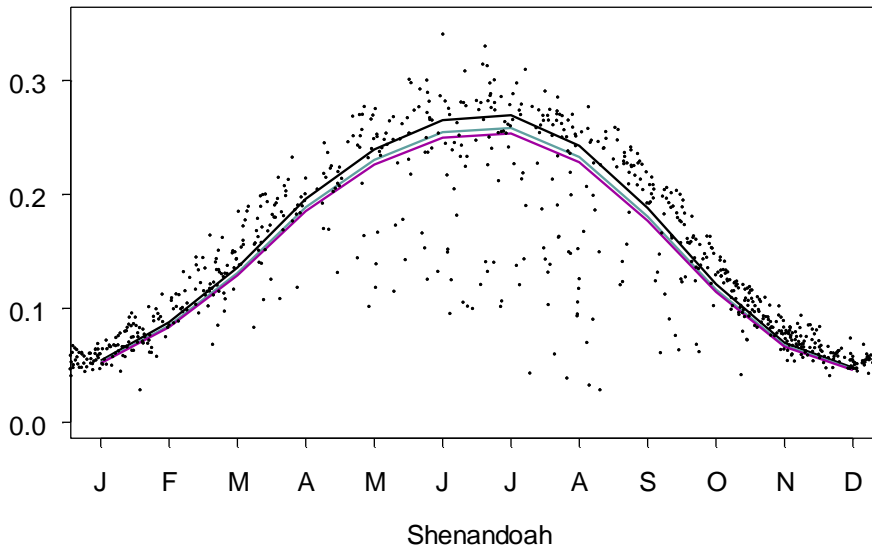
Sequoia and King's Canyon National Parks cover 800,000 acres in the western United States. The effects of ozone pollution are illustrated by the three curves in the above figure: the black curve corresponds to modeled UV irradiances for 0 ppb surface ozone, the blue curve represents the modeled irradiance for 80 ppb surface ozone, and the purple curve corresponds to the modeled irradiance for 120 ppb surface ozone. As ozone concentration increases, the amount of UV irradiance reaching the surface decreases. The comparison assumes that all other values are held constant, which is not the case for the Brewer UV measurements, plotted as the small symbols in the figure. The scatter in the points confirms that many factors besides pollution affect UV reaching the surface, and suggests that the overall effects of pollution on UV irradiances are not large.

# Shenandoah National Park

Latitude: 38.5°N  
Longitude: 78.4°W  
Elevation: 325 m



## Influence of High Pollution Levels on Noontime UV



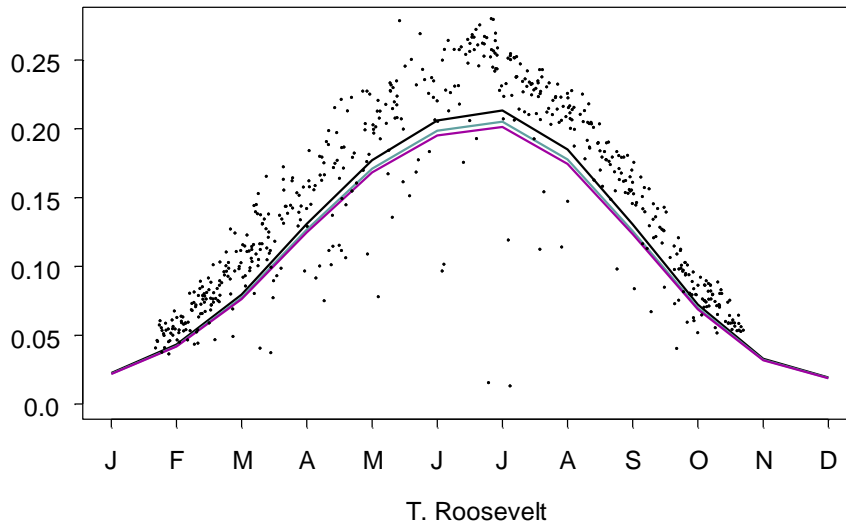
Shenandoah National Park covers roughly 200,000 acres in the eastern U.S. The UV values over time indicate generally low variability. The effects of ozone pollution are illustrated by the three curves in the above figure: the black curve corresponds to modeled UV irradiances for 0 ppb surface ozone, the blue curve represents the modeled irradiance for 80 ppb surface ozone, and the purple curve corresponds to the modeled irradiance for 120 ppb surface ozone. As ozone concentration increases, the amount of UV irradiance reaching the surface decreases. The comparison assumes that all other values are held constant, which is not the case for the Brewer UV measurements, plotted as the small symbols in the figure. The scatter in the UV data confirms that many factors besides pollution affect UV reaching the surface. The overall effects of pollution on UV irradiances are not large compared to the effects of Sun angle, clouds, and other factors.

# Theodore Roosevelt National Park



Latitude: 46.9°N  
Longitude: 103.4°W  
Elevation: 238 m

## Influence of High Pollution Levels on Noontime UV



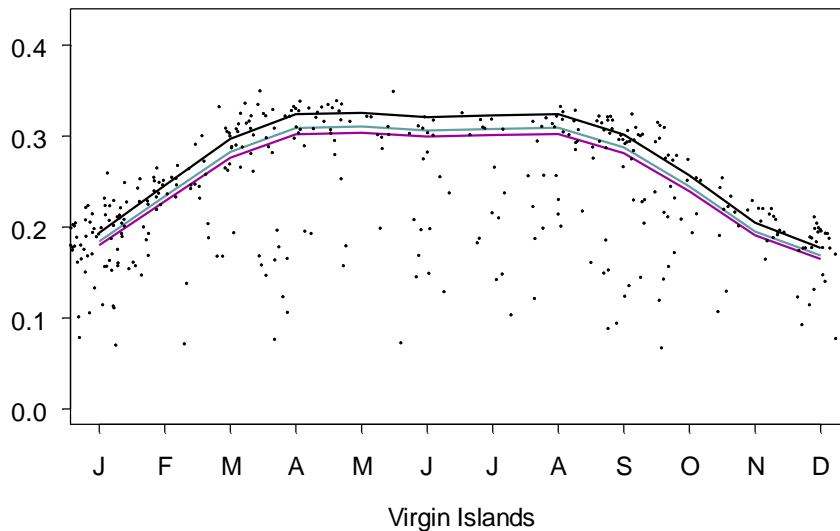
Theodore Roosevelt National Park, with an area of 70,000 acres, is located in North Dakota on the high Northern Plains. The effects of ozone pollution are illustrated by the three curves in the above figure: the black curve corresponds to modeled UV irradiances for 0 ppb surface ozone, the blue curve is modeled irradiance for 80 ppb surface ozone, and the purple curve is modeled irradiance for 120 ppb surface ozone. As ozone concentration increases, the amount of UV irradiance reaching the surface decreases. The comparison assumes that all other values are held constant, which is not the case for the Brewer UV measurements, also plotted in the figure. The scatter in the points confirms that many factors besides pollution affect UV reaching the surface. Overall, the overall effects of pollution on UV irradiances are not large.

# Virgin Islands National Park

Latitude: 18.3°N  
Longitude: 64.8°W  
Elevation: 30 m



### Influence of High Pollution Levels on Noontime UV



Virgin Islands National Park is the most southern location in the EPA network. The Brewer instrument is located within the tropics and the data therefore exhibit a rather unusual seasonal cycle. The effects of ozone pollution are illustrated by the three curves in the above figure: the black curve corresponds to modeled UV irradiances for 0 ppb surface ozone, the blue curve is the modeled irradiance for 80 ppb surface ozone, and the purple curve is the modeled irradiance for 120 ppb surface ozone. As ozone concentration increases, the amount of UV irradiance reaching the surface decreases. The comparison assumes that all other values are held constant, which is not the case for the Brewer UV measurements, also plotted in the figure. The scatter in the points confirms that many factors besides pollution affect UV reaching the surface. Many of these other factors affect UV much more strongly than the effects from pollution.

## 5. Intercomparison of Results for All 21 Brewer Locations

Table 2 reports the percent reduction in UV for each site within the network. The percent reduction of a comparison of 80 ppb of ozone in the boundary layer to 0 ppb of ozone in the boundary layer is given by season in columns c through f, and for the entire year in column g. This comparison suggests the maximum attenuation of UV by boundary layer ozone amounts. In reality, 0 ppb of ozone is never observed, so the percentages reported here are a comparison to an ideal, very clean state, and are therefore high. Typical background ozone levels can range from 10 ppb to 40 ppb and higher at some locations.

Table 2. Percent reduction in UV irradiance by 80 ppb ozone, compared to a surface ozone amount of 0 ppb. Results are reported for each season and for the entire year.

	(a)	(b)	(c)	(d)	(e)	(f)	(g)
	Lat.	Elev.	Winter	Spring	Summer	Autumn	Annual
<b>Acadia</b>	44.4	137	2.21	3.21	3.86	3.34	3.15
<b>Albuquerque</b>	35.1	1615	2.86	3.15	3.46	3.38	3.21
<b>Atlanta</b>	33.8	91	3.45	3.86	4.23	4.10	3.91
<b>Big Bend</b>	29.3	329	3.57	3.78	4.09	4.09	3.88
<b>Boulder</b>	40.1	1689	2.14	2.69	3.16	2.98	2.74
<b>Canyonlands</b>	38.5	814	2.93	3.49	3.82	3.59	3.46
<b>Chicago</b>	41.8	165	2.40	3.24	3.87	3.46	3.24
<b>Denali</b>	63.7	661	0.72	2.14	3.17	1.79	1.96
<b>Everglades</b>	25.4	18	4.42	4.40	4.44	4.51	4.44
<b>Gaithersburg</b>	39.1	43	3.13	3.82	4.20	3.90	3.76
<b>Glacier</b>	48.7	424	1.83	3.00	3.65	3.02	2.87
<b>Great Smoky</b>	35.6	564	3.18	3.62	3.97	3.81	3.64
<b>Hawaii</b>	19.4	1243	4.15	4.02	3.92	4.01	4.03
<b>Olympic</b>	48.1	32	1.96	3.18	3.86	3.16	3.04
<b>R.T.P</b>	35.9	104	3.32	3.83	4.20	4.02	3.84
<b>Riverside</b>	34.0	84	3.44	3.86	4.21	4.08	3.90
<b>Rocky Mountain</b>	40.0	2896	1.88	2.31	2.68	2.57	2.36
<b>Sequoia</b>	36.5	549	3.13	3.61	3.94	3.77	3.61
<b>Shenandoah</b>	38.5	325	3.07	3.69	4.07	3.82	3.66
<b>T. Roosevelt</b>	46.9	238	2.01	3.15	3.76	3.17	3.02
<b>Virgin Islands</b>	18.3	30	4.83	4.70	4.59	4.69	4.70
<b>Network Mean</b>			<b>2.89</b>	<b>3.46</b>	<b>3.86</b>	<b>3.58</b>	<b>3.45</b>

Figure 7 illustrates the percent attenuation of noontime clear sky CIE-weighted UV for all 21 Brewer locations. The results are based on radiative transfer calculations using actual observed total column ozone values. These plots show that boundary layer ozone

has its largest effects at high Sun angles, experienced near the tropics and during local summer.

## Influence of High Pollution Levels on Noontime UV

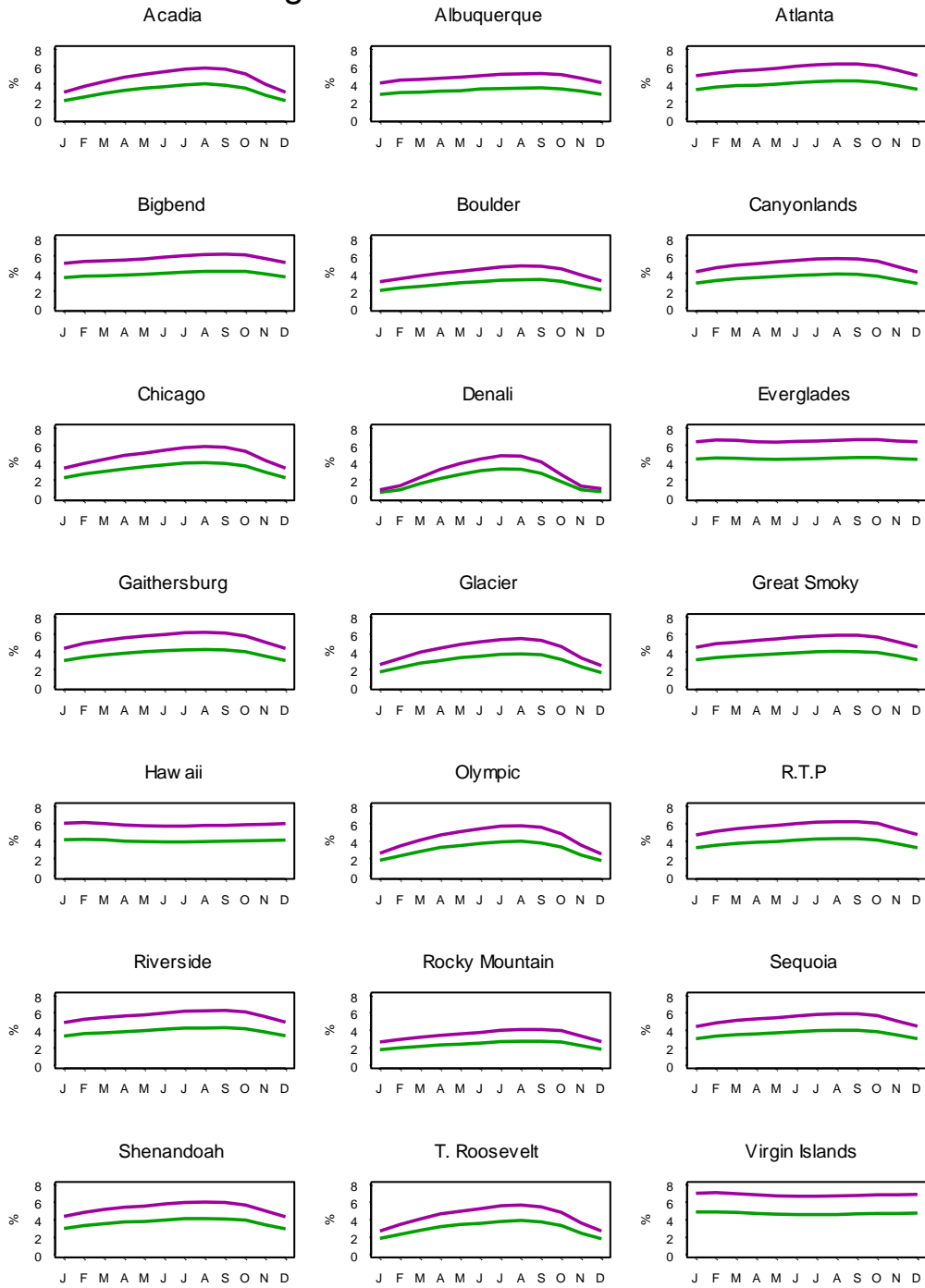


**Figure 7. UV attenuation by 80 ppb ozone (green line) and 120 ppb ozone (purple line) is plotted as a function of time of year for all 21 Brewer locations.**

The percent UV attenuation for each season as a function of elevation is shown in Figure 8. Overall, there appears to be a slight decrease in the percent attenuation as elevation increases. The reduction in yearly-averaged noontime CIE is plotted as a function of elevation in Figure 9. For the 21 Brewer sites, there appears to be a diminished influence of pollutants at higher elevations for estimates of clear sky UV. This diminishment is partially due to the reference levels of ozone, which are specified in parts per billion. With higher elevation, and therefore lower atmospheric density, 80 ppb of ozone represents fewer ozone molecules to absorb UV.

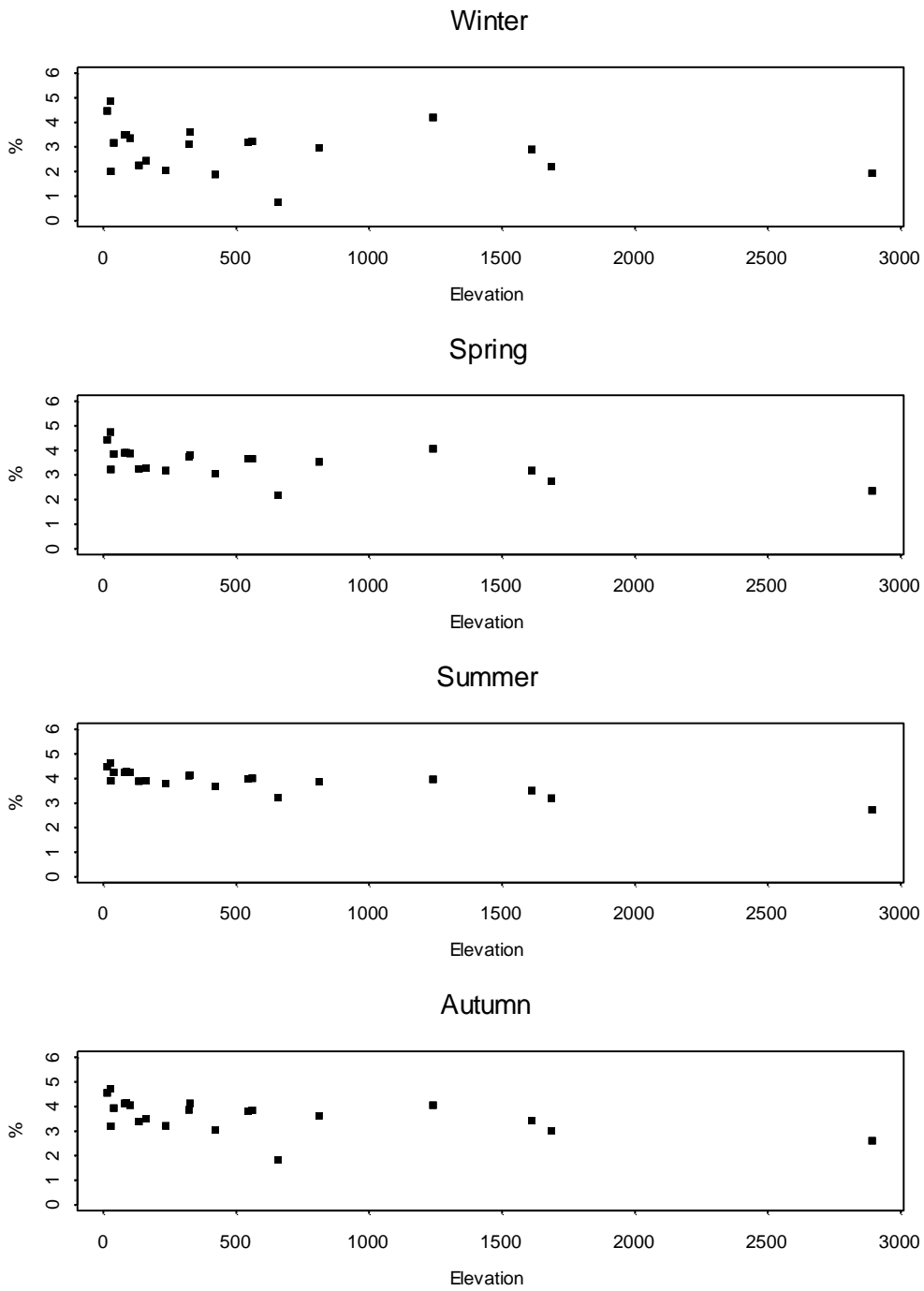


**Figure 8. Percent attenuation of UV irradiance by 80 ppb ozone, plotted for each season as a function of elevation.**

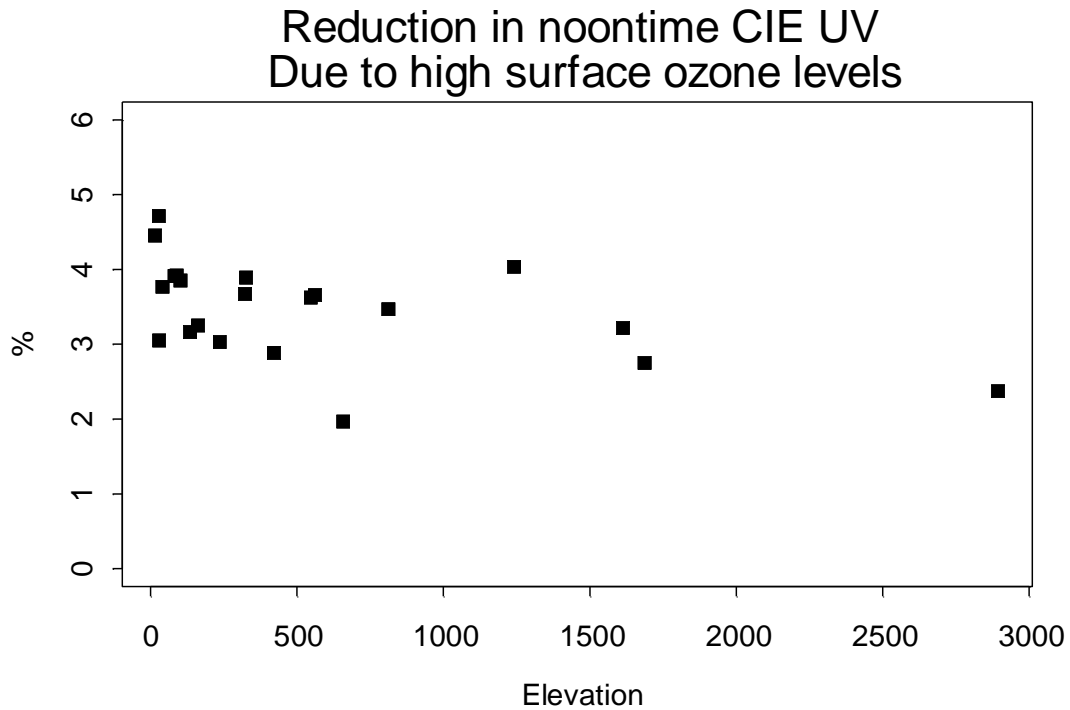


**Figure 9. Percent reduction in yearly-averaged noontime CIE UV due to 80 ppb ozone, plotted as a function of elevation.**

The next figures illustrate the percent attenuation of UV irradiance as a function of latitude. The symbols represent the percent attenuation of UV due to 80 ppb surface ozone, compared to simulations in which 0 ppb surface ozone was included. Overall, the percent attenuation is highest at the lowest latitudes, where the Sun tends to be highest in the sky.

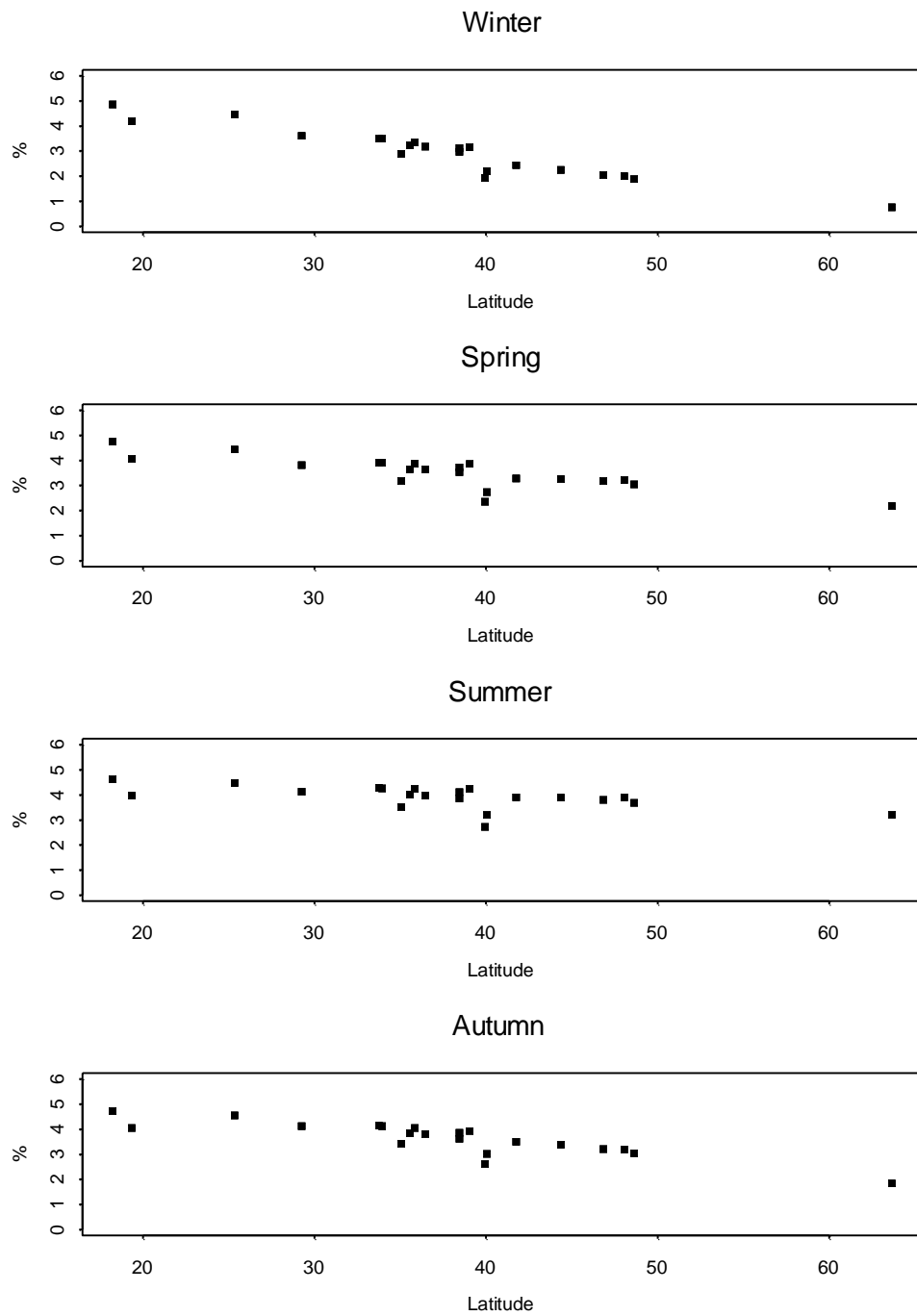


**Figure 10. Percent attenuation of UV irradiance by 80 ppb ozone, plotted as function of latitude.**

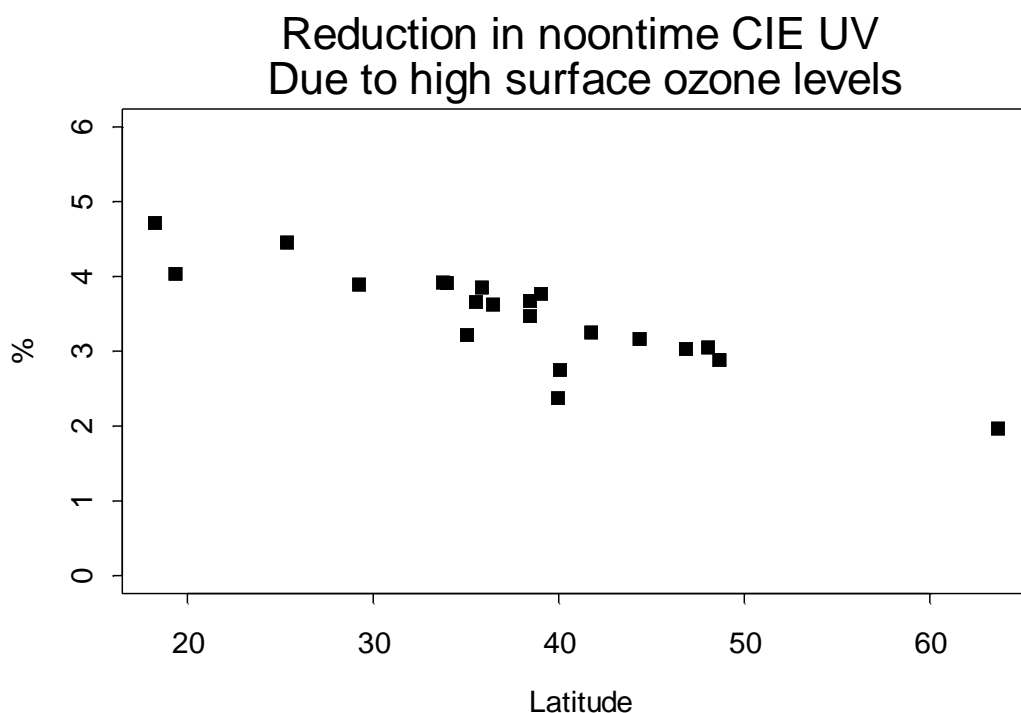


**Figure 11. Percent attenuation of yearly-averaged noontime CIE UV due to 80 ppb ozone, plotted as a function of latitude.**

## 6. Conclusion

Ultraviolet radiation from the sun is scattered and absorbed by the atmosphere. Stratospheric ozone, clouds, and molecular scattering attenuate UV as it transverses the atmosphere. Ozone near the surface can also attenuate UV, though because of the small concentrations of ozone found in the lowest part of this atmosphere, the attenuation due to elevated surface ozone is generally less than 5 percent. Measurements from the Brewer network and radiative transfer calculations are used in this report to estimate the effects of pollutants on surface UV. Because of the importance of surface ozone and the availability of data, we focus on the effects of tropospheric ozone on UV transmission.

The U.S. EPA has set air quality standards for ozone exposure during 8-hour and 1-hour periods. The 8-hour standard is 0.08 ppm (80 ppb), and locations are able meet attainment based on the three-year average of the 4th highest daily concentration. The 1-hr standard, which is being replaced with the 8-hr standard in most areas, is 0.12 ppm (120 ppb). These limits are based on knowledge that excess ozone amounts can be

detrimental to human health, to plants and to other biological processes. Exposure to high ozone levels is known to cause damage to human lungs, and can be particularly problematic for people with asthma or other respiratory conditions. High ozone in the boundary layer can also affect rubber products and other materials.

The question of how much UV is attenuated by surface ozone is difficult to answer for a number of reasons. The measurements of both UV and surface ozone are difficult and high accuracy is needed to verify small effects. Days of high ozone are often days when other atmospheric changes are taking place, including changes in cloud cover and heights of boundary layer conditions, all of which can affect UV either directly or indirectly. Furthermore, strong diurnal cycles in both UV and pollutants result in the highest pollution levels being observed in the afternoon, when UV is already waning.

Analysis of collocated EPA Brewer measurements and surface ozone measurements for Chicago, Illinois, show a negative correlation between the two, substantiating the concept that higher surface pollution can reduce the UV levels reaching the ground. Analyzing the Brewer data by wavelength shows an attenuation of 5 percent at the lowest wavelengths (305 nm) and an attenuation of 3 percent at the longer wavelengths (315 nm). This spectral dependence of the attenuation is further evidence that the UV attenuation is caused by ozone in the lower atmosphere, rather than by other atmospheric parameters such as clouds or aerosols.

Radiative transfer calculations were performed for all 21 EPA Brewer locations using measured ozone values. Two high pollution situations were considered, corresponding to 80 ppb and 120 ppb of ozone in the lowest part of the atmosphere. For the model calculations, it was estimated that these levels existed throughout a 1.5-km thick boundary layer. The results of these calculations were compared to calculations that assumed no (0 ppb) boundary layer ozone. This comparison allows us to estimate the maximum effects of ozone in the lower atmosphere. The results across the network suggest that UV is generally attenuated by less than 5 percent for high ozone concentrations of 80 ppb. The attenuation is highest in the summer, with a network average of 3.9 percent, and lowest in the winter, with a network average of 2.9 percent for 120 ppb and 80 ppb respectively.

## Some references relevant to interpretation of UV data

- Bartlett, L.M. and A.R. Webb, Changes in ultraviolet radiation in the 1990s: Spectral measurements from Reading, England, *J. Geophys. Res.*, 105, 4889-4893, 2000.
- Barnard, W. F., V. K. Saxena, B. N. Wenny and J. DeLuisi, Daily surface UV exposure and its relationship to surface pollutant measurements. AWMA, 2003.
- Bhartia, P.K., J. Herman, R.D. McPeters, and O. Torres, 1993. The effect of Mt. Pinatubo aerosols on total ozone measurements from backscatter ultra violet (BUV) Experiments. *J. Geophys. Res.*, 98, 18547-18554.
- Bodhaine, B.A., E.G. Dutton, R.L. McKenzie, and P.V. Johnston, Calibrating broadband UV instruments: Ozone and solar zenith angle dependence, *J. Atmos. Oceanic Technol.*, 15, 916-926, 1998.
- Bowman, K.P., 1986, Interannual variability of total ozone during the breakdown of the Antarctic circumpolar vortex, *Geophys. Res. Lett.*, 13, 1193-1196.
- Bowman, K.P., 1988, Global trends in total ozone, *Science*, 239, 48-50.
- Bruel, C., and P. J. Crutzen (1989), On the disproportionate role of tropospheric ozone as a filter against solar UV-B radiation, *Geophys. Res. Lett.*, 16, 703-706.
- Casale, G.R., D. Meloni, S. Miano, S. Palmieri, A.M. Siani, and F. Cappellani, Solar UV-B irradiance and total ozone in Italy: Fluctuations and trends, *J. Geophys. Res.*, 105, 4895-4901, 2000.
- Commission Internationale de l'Eclairage (CIE), Erythema Reference Action Spectrum and Standard Erythema Dose. Joint ISO/CIE Standard, ISO 17166:1999/CIE S007-1998, 1998.
- Dave, J.V. 1964. Meaning of successive iteration of the auxiliary equation of radiative transfer. *Astrophys. J.*, 140, 1292-1303.
- Dave, J.V. 1978, Effect of aerosols on the estimate of total ozone in an atmospheric column from the measurements of its ultraviolet radiance, *J. Atmos. Sci.*, 35, 899-911.
- Disterhoft, G. Fiocco, D. Fua, and F. Monteleone, Effects of desert dust and ozone on the ultraviolet irradiance at the Mediterranean Island of Lampedusa during PAUR II, *J. Geophys. Res.*, 107(D18), 8135, 2002.
- Eck, T.F., P.K. Bhartia, and J.B. Kerr, 1995, Satellite estimation of spectral UVB irradiance using TOMS derived total ozone and UV reflectivity, *Geophys. Res. Lett.*, 22(5), 611-614.
- Erlick, C. and J. E. Frederick, The effects of aerosols on the wavelength dependence of atmospheric transmission in the ultraviolet and visible, Part I: A "single scattering separate" delta-Eddington model, *J. Geophys. Res.*, 103, 11,465-11,472, 1998.

- Erlick, C. and J. E. Frederick, The effects of aerosols on the wavelength dependence of atmospheric transmission in the ultraviolet and visible, Part II: Typical continental and urban aerosols in clear skies, *J. Geophys. Res.*, 103, 23,275-23,285, 1998.
- Erlick, C., J. E. Frederick, V., K. Saxena, and B. N. Wenny, Atmospheric transmission in the ultraviolet and visible: Aerosols in cloudy atmospheres, *J. Geophys. Res.*, 103, 31,541-31,556, 1998.
- Estupiñán, J.G., S. Raman, G.H. Crescenti, J.J. Streicher, and W.F. Barnard, Effects of clouds and haze on UV-B radiation, *J. Geophys. Res.*, 101, 16807-16816, 1996.
- Fioletov, V.E., L.J.B. McArthur, J.B. Kerr, and D.I. Wardle, Long-term variations of UV-B irradiance over Canada estimated from Brewer observations and derived from ozone and pyranometer measurements, *J. Geophys. Res.*, 106, 23009-23027, 2001.
- Frederick, J. E. and C. Erlick (1995), Trends and interannual variations in erythemal sunlight, 1978-1993, *Photochem. Photobiol.* 62, 476-484.
- Gordon, H.R., and D.K. Clark, 1981, Clear water radiances for atmospheric correction of Coastal Zone Color Scanner imagery, *Appl. Optics*, 20, 4175-4180.
- Grant, R.H. and G.M. Heisler, Estimation of ultraviolet-B irradiance under variable cloud conditions, *J. Appl. Meteorol.*, 39, 904-916, 2000.
- Ilyas, M., A. Pandey, and M.S. Jaafar, Changes to the surface level solar ultraviolet-B radiation due to haze perturbation, *J. Atmos. Chem.*, 40, 111-121, 2001.
- Jacobson, M.Z., Global direct radiative forcing due to multicomponent anthropogenic and natural aerosols, *J. Geophys. Res.*, 106, 1551-1568, 2001.
- Josefsson, W. and T. Landelius, Effects of clouds on UV irradiance: As estimated from cloud amount, cloud type, precipitation, global radiation and sunshine duration. *J. Geophys. Res.*, 105, 4927-4935, 2000.
- Kerr, J.B., Automated Brewer spectrophotometer, in *Proceedings of the 4<sup>th</sup> Ozone Symposium on Atmospheric Ozone*, pp. 396-401, D. Reidel, Norwell, Mass., 1985.
- Kerr, J.B. and McElroy, C.T. 1993. Evidence for large upward trends of ultraviolet-B radiation linked to ozone depletion. *Science* 262:1032-1034.
- Kirchoff, V.W.J.H., A.A. Silva, C.A. Costa, N. Paes Leme, H.G. Pavao, and F. Zaratti, UV-B optical thickness observations of the atmosphere, *J. Geophys. Res.*, 106, 2963-2973, 2001.
- Klenk, K.F., P.K. Bhartia, A.J. Fleig, V.G. Kaveeshwar, R.D. McPeters, and P.M. Smith, 1982, Total ozone determination from the Backscattered Ultraviolet (BUV) Experiment, *J. Appl. Meteor.*, 21, 1672-1684.

- Lait, L.R., M.R. Schoeberl, and P.A. Newman, 1989, Quasi-biennial modulation of the Antarctic ozone depletion, *J. Geophys. Res.*, 94, 559-571.
- Lienesch, J.H., and P.K.K. Pardey, 1985, "The use of TOMS data in evaluating and improving the total ozone from TOVS measurements", Rep. NOAA-TR-NESDIS-23, Issue 22, 3814-3828.
- Liou, K.-N., 1980, *An Introduction to Atmospheric Radiation*, Academic Press, New York.
- Long, C.S., Miller, A.J., H-T. Lee, J.D. Wild, R.C. Przywarty, D. Hufford, Ultraviolet Index Forecasts Issued by the National Weather Service. *Bull. Amer. Meteorol. Soc.*, 77, 729-748, 1996.
- Long, C.S., UV Index Forecasting Practices around the World, in SPARC Newsletter 21, June 2003.
- McArthur, L.J.B., V.E. Fioletov, J.B. Kerr, C.T. McElroy, and D.I. Wardle, Derivation of UV-A irradiance from pyranometer measurements, *J. Geophys. Res.*, 104, 30139-30151, 1999.
- McKenzie, R.L. et al., Increased summertime UV radiation in New Zealand in response to ozone loss, *Science*, 285, 1709-1711, 1999.
- McKenzie, R.L. et al., Satellite retrievals of erythemal UV dose compared with ground-based measurements at northern and southern midlatitudes, *J. Geophys. Res.*, 106, 24,051-24,062, 2001.
- McKinlay A.F. and B.L. Diffey, A reference action spectrum for ultraviolet induced erythemal in human skin, *CIE J.*, 6, 17-22, 1987.
- McPeters, R., and W.D Komhyr. 1991. Long-term changes in the Total Ozone Mapping Spectrometer relative to world standard Dobson Spectrometer 83. *J. Geophys. Res.*, 96, 2987-2993.
- McPeters, R.D., P.K. Bhartia, A.J. Krueger, J. R. Herman, B. Schlesinger, C.G. Wellemeyer, C. J. Seftor, G. Jaross, S.L. Taylor, T. Swissler, O. Torres, G. Labow, W. Byerly, and R.P. Cebula, 1996. *Nimbus-7 Total Ozone Mapping Spectrometer (TOMS) Data Products User's Guide*. NASA Reference Publication 1384.
- Miller, A.J., R.M. Nagatani, K.B. Labitzke, E. Klinker, K. Rose, and D.F. Heath, 1976, Stratospheric ozone transport during the mid-winter warming of December 1970-January 1971, paper presented at Joint Symposium on Atmospheric Ozone, Dresden, Germany, August 9-16, 1976.
- Molina, L. T., and M. J. and Molina (1986), Absolute absorption cross sections of ozone in the 185- to 350- nm wavelength range, *J. Geophys. Res.*, 91, 14,501-14,508.
- Newchurch, M.J. et al., Evidence for slowdown in stratospheric ozone loss: First stage of ozone recovery, *J. Geophys. Res.*, 108, 4507, 2003.

- Pappayannis, A., D. Balis, A. Bais, H. van der Bergh, B. Calpini, E. Durieux, L. Fiorani, L. Jaquet, I. Ziomas, and C.S. Zerefos, Role of urban and suburban aerosols on solar UV radiation over Athens, Greece, *Atmos. Environ.*, 32(12):2193-2201, 1998.
- Reinsel, G.C. et al., On detection of turnaround and recovery in ozone, *J. Geophys. Res.*, 107(D10):4078, 2002.
- Reinsel, G.C. et al., Trend analysis of total ozone data for turnaround and dynamical contributions, *J. Geophys. Res.*, submitted, 2004.
- Renaud, A., J. Staehelin, C. Frohlich, R. Philipona, and A. Heimo, Influence of snow and clouds on erythemal UV radiation: Analysis of Swiss measurements and comparisons with models, *J. Geophys. Res.*, 105, 4961-4969, 2000.
- Repapis, C.C., H.T. Mantis, A.G. Paliatsos, C.M. Philandras, A.F. Bais, and C. Meleti, Case study of UV-B modification during episodes of urban air pollution, *Atmos. Environ.*, 32(12):2203-2208, 1998.
- Sabburg, J. and J. Wong, The effect of clouds on enhancing UV-B irradiance at the Earth's surface: A one-year study, *Geophys. Res. Lett.*, 27, 3337-3340, 2000.
- Schwander, H., P. Koepke, A. Kaifel, and G. Seckmeyer, Modifications of spectral UV irradiance by clouds, *J. Geophys. Res.*, 107(D16), 4296, 2002.
- Tarasick, D.W., Fioletov, V.E., Wardle, D.I., Kerr, J.B., McArthur, J.B., McLinden, C.A. Climatology and trends in surface UV radiation -- survey article. *Atmosphere-Ocean*, vol. 41, no. 2, pp. 121-138, 2003.
- United Nations Environment Programme, Environmental Effects of Ozone Depletion, *Journal of Photochemistry and Photobiology B: Biology*, November 1998.
- Weatherhead, E. C. and A. R. Webb, 1997: International Response to the Challenge of Measuring Solar Ultraviolet Radiation. *Radiation Protection Dosimetry-Non-Ionising Radiation*, 72, 223-229.
- Weatherhead, E. C., G. C. Reinsel, G. C. Tiao, X. Meng, D. Choi, W. Cheang, T. Keller, J. DeLuisi, D. J. Wuebbles, J. B. Kerr, A. J. Miller, S. J. Oltmans, and J. E. Frederick, Factors affecting the detection of trends: Statistical considerations and applications to environmental data. *Journal of Geophysical Research*, 103, 17149-17161, 1998.
- Weatherhead, E. C., G. C. Reinsel, G. C. Tiao, C. H. Jackman, L. Bishop, S. M. H. Frith, J. DeLuisi, T. Keller, S. Oltmans, E. Fleming, D. Wuebbles, J. Kerr, A. Miller, J. Herman, R. McPeters, R. Nagatani, and J. Frederick, 2000: Detecting the Recovery of Total Column Ozone. *Journal of Geophysical Research*, 105, 22201-22210.
- Weatherhead, E.C. et al., Temperature dependence of the Brewer ultraviolet data. *J. Geophys. Res.*, 106, 34,121-34,129, 2001.

- Weihs, P., A.R. Webb, S.J. Hutchinson, and G.W. Middleton, Measurements of the diffuse UV sky irradiance during broken cloud conditions, *Journal of Geophysical Research.*, 105, 4937-4944, 2000.
- Wenny, B. N., Saxena, V. K., Frederick J. E., Aerosol optical depth measurements and their impact on surface levels of Ultraviolet-B radiation, *Journal of Geophysical Research* 106(D15) 17311-17325, 2001.
- Winiecki, Shelby and John E. Frederick, Ultraviolet radiation and clouds: Couplings to tropospheric air quality", *Journal of Geophysical Research-Atmospheres*, 110, doi:10.1029/2005JD006199, 2005.
- World Health Organization (WHO), Global Solar UV Index : A Practical Guide. A Joint Recommendation of the World Health Organization, World Meteorological Organization, United Nations Environment Programme, and International Commission on Non-Ionizing Radiation Protection, 2002.
- World Meteorological Organization (WMO), Scientific Assessment of Ozone Depletion: 1998, Global Ozone Research and Monitoring Project—Report No. 44, Geneva, 1999.
- World Meteorological Organization (WMO), Scientific Assessment of Ozone Depletion: 2002, Global Ozone Research and Monitoring Project—Report No. 47, 498 pp., Geneva, 2003.